THE ROLE OF IL-1R8 IN MODULATING MACROPHAGE INFLAMMATION: IMPLICATIONS FOR ATHEROSCLEROSIS

A THESIS SUBMITTED TO THE GRADUATE DIVISION OF THE UNIVERSITY OF HAWAI‘I AT MANOA IN PARTIAL FULFILLMENT OF THE REQUIREMENTS FOR THE DEGREE OF

MASTER OF SCIENCE

IN

MOLECULAR BIOSCIENCES & BIOENGINEERING

JULY 2017

BY CHLOE A. LIU

Thesis Committee:

William A. Boisvert, PhD, Chairperson
Takashi Matsui, MD, PhD
Jun Panee, PhD

ACKNOWLEDGEMENTS

I would like to acknowledge and sincerely thank my master's advisor, Dr. William A. Boisvert, for supporting my research and being an excellent mentor. You have been instrumental in guiding me through my thesis research and have been a positive influence on my career goals. I would also like to thank Dr. Takashi Matsui and Dr. Jun Panee for their mentorship and serving on my committee.

Thank you to Dr. Sara McCurdy for mentoring me from day one. I am so grateful to have such a knowledgeable, supportive, and patient, post-doctoral mentor. Without your unwavering dedication to support me and the lab, my thesis would not have been accomplished. You will be successful in your next journey in San Diego and I am happy to have been under your guidance.

I would like to thank my MBBE Master's Graduate Chair, Dr. Jon Paul Bingham, for his guidance for the last two years. Thank you for going above and beyond what is required of a professor and implementing enriching programs like the CTAHR Research Symposium and 3MEP (3 Minute Presentation) Competition.

I would also like to thank my Lab Ohana for their support and comradery over the last two years. A special thanks to my lab mates, Jonathan Yap, Jan Garo, Martin Alcala, and Whitney Regan. Every day in lab was a learning experience and I am thankful to have you all to support me. I would like to thank Karolina Peplowska and Maarit Tiirikainen with the UH Cancer Genomics Shared Resource Core. And Dr. Megan Porter and Ms. Cheryl Squair for allowing me to TA general and cell molecular biology. Students, I wish you all the best.

Lastly, I would like to thank my parents, siblings, and grandparents for their love and support on my journey to pursue my dream. I also wanted to thank my MBBE and CMB crew for their support, nerdy conversations, and coffee breaks. Mahalo.

ABSTRACT

Atherosclerosis is a chronic inflammatory disease of the cardiovascular system characterized by macrophage-driven arterial plaque accumulation. Interleukin (IL)-37 is an anti-inflammatory cytokine within the IL-1 family which suppresses inflammatory immune response by complexing with the receptors IL-1R8 and IL-18Rα. Because IL-37 and its receptor are robustly expressed in the macrophage, I sought to determine if IL-1R8 plays a key role in macrophage inflammation that may in turn influence the development of atherosclerosis.

Initially the proposed anti-inflammatory effects of IL-37 was investigated by co-treating mice bone marrow-derived macrophages (BMDM) with recombinant IL-37 protein and various inflammatory stimuli. Although inflammation was not quelled by IL-37, interestingly, IL-1R8 was consistently downregulated by LPS and IFNγ treatment. To test whether IL-1R8 inhibits inflammation, I overexpressed IL-1R8 in the mouse macrophage cell line, RAW 264.7 cells, and BMDM by transfection with IL-1R8 or GFP expression plasmids. Transfected cells were treated with pro-inflammatory (LPS, IFNγ, TNFα) or anti-inflammatory (IL-4) mediators, as well as IL-37. Transfection of RAW 264.7 cells with IL-1R8 resulted in 35-to-60-fold increases of IL-1R8 transcript expression compared to controls as measured by RT-qPCR, whereas IL-1R8 protein level was increased 6 to9 folds compared to GFP-transfected control cells, as measured by Western blot. Interestingly, transfection with IL-1R8 resulted in robust overexpression of IL-1R8 with a molecular weight of 70-95 kDa, indicating significant glycosylation, which was confirmed by glycosidase treatment. In contrast to my initial hypothesis, overexpression of IL-1R8 in RAW cells and BMDM had a pro-inflammatory effect overall. However, when treated with recombinant IL-37 protein as the ligand for IL-1R8, the IL-1R8-transfected RAW cells showed reduced inflammatory gene expression compared to GFP controls treated with the same stimulus.

Additionally, siRNA knockdown of IL-1R8 resulted in significantly higher inflammatory gene expression, such as IL-6, IL-1b, iNOS, MCP1/CCL2, and TNFα in both RAW 264.7 cells and BMDM. The experiments described show that IL-1R8, along with its ligand IL-37, plays a role in regulating macrophage inflammation, although future studies are needed to further elucidate its exact molecular mechanism.

TABLE OF CONTENTS

LIST OF FIGURES

LIST OF TABLES

LIST OF ABBREVIATIONS

apoB-LP: apolipoprotein B-containing lipoproteins

BMDM: bone marrow derived macrophages

°C: degree Celsius

CMV: Cytomegalovirus

CVD: cardiovascular disease

DMEM: Dulbecco's modified eagle medium

DMSO: Dimethyl sulfoxide

EDTA: ethylenediaminestetraacetate

GFP: Enhanced green fluorescent protein

ER: endoplasmic reticulum

FBS: fetal bovine serum

FH: familial hypercholesterolemia

HEPES: 2-[4-(2-hydroxyethyl) piperazin-1-yl] ethanesulfonic acid

IL-37: Interleukin -1 family cytokine 37

IL-18bp: IL-18 binding protein

IL-1Rα: IL-1 receptor antagonist

LDL: low density lipoprotein

LDLR: low density lipoprotein receptor

LPS: lipopolysaccharide

MI: myocardial infarction

PBMC: peripheral blood mononuclear cells

PBS: phosphate buffered saline

PCR: Polymerase Chain Reaction

RT-qPCR: Reverse transcriptase quantitative PCR

SIGIRR: Single Immunoglobulin Interleukin-1 Related Receptor

Tg: Transgenic

TIR8: Toll/Interleukin-1 Receptor 8

CHAPTER 1: INTRODUCTION

1. Cardiovascular Disease and Atherosclerosis

Cardiovascular diseases (CVD) are the leading cause of death, accounting for 17.7 million deaths or 31% of total deaths in the world in 2015 [1, 2]. Central Asia, Eastern Europe, and developing countries have the highest death rate due to CVD [2]. The high percentage of deaths in developing countries contributed to a total estimated economic burden of $863 billion in 2015 [3, 4]. The American Heart Association reports that in the United States (US), approximately 801,000 people die from heart disease annually, which is equivalent to 1 in every 3 deaths [5, 6]. The distribution of deaths in the US due to cardiovascular disease is shown in **Figure 1** [7]. In 2015, 41.5% (102.7 million) of the US population had at least one CVD condition. In 2016, the approximate total US economic burden was $555 billion, and is projected to increase to $1.1 trillion by 2035 [8]. CVD is comprised of a group of heart and blood vessel diseases, the most common of which include: hypertension, coronary heart disease, stroke, congestive heart failure, and atrial fibrillation [1, 6]. Since atherosclerosis is the leading cause of CVD, it is important that we understand the macrophage-driven inflammatory mechanisms that drive its pathogenesis [3]. Developing novel, targeted therapies will help to prevent deaths and reduce the global economic burden due to CVD.

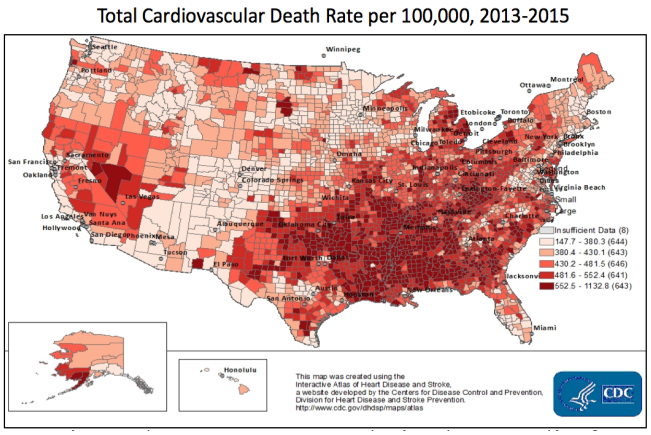

Figure 1. Map of the total CVD death rate in the United States from 2013-2015, including all races and both sexes. The CDC Interactive Atlas of Heart Disease and Stroke reports the incidence of death due to CVD ranging from 147.7-1132.8 per 100,000 people (adapted by the author of this thesis) [7].

1.1. Atherosclerosis Causes and Risk Factors

Atherosclerosis was once believed to be a disease caused largely by lipid accumulation in the arteries, but it is now understood to be a chronic inflammatory disease involving the immune system, particularly monocytes and macrophages. There are major modifiable risk factors that contribute to atherosclerosis development, which includes, hyperlipidemia due to an elevated circulating low density lipoprotein (LDL); hypertension; tobacco and alcohol usage; obesity; unhealthy diet; and physical inactivity. There are also non-modifiable risk factors which includes, aging, gender, ethnicity, and family history.

Most of these aforementioned risk factors are environmental, but some are inherited or acquired genetic mutations that can predispose patients to atherosclerosis development. For example, homozygous familial hypercholesterolemia (FH), which occurs in 1 out of 1,000,000 people, is caused by a mutation in both copies of the low-density lipoprotein receptor (LDLR) gene that prevents LDLR expression in the liver. More commonly, about 1 in 500 people have a heterozygous mutation which results in approximately 50% reduction in the expression of LDLR. Both mutations prevent LDL uptake via LDLR and increases total circulating cholesterol [9]. Both environmental and genetic factors can contribute to increased lipid accumulation and immune cell infiltration within the arterial wall, leading to plaque formation and atherosclerosis over time [3, 10].

1.2. The role of macrophages in atherosclerosis development

In human and mouse models, early stage atherosclerosis begins with the formation of a fatty streak lesion, due to the accumulation of apolipoprotein B-containing lipoproteins (apoB-LPs) in the sub-endothelial space. Leukocytes, especially monocytes, are attracted to sites of vascular inflammation and transmigrate through the endothelial monolayer where they

differentiate into macrophages [11, 12]. As the atherosclerotic lesion develops, vascular smooth muscle cells are activated and migrate to form a protective layer called the fibrous cap, which is rich in extracellular matrix fibers (e.g., collagen), and prevents the blood from coming in contact with the inflammatory and thrombotic elements of the necrotic core. The necrotic core consists of dead cells, lipid deposits, and other inflammatory debris. In the intermediate stage, macrophages in the intima take up modified lipoproteins and become foam cells. The accumulation of apoptotic lipoproteins and impaired phagocytic clearance results in the formation of a necrotic core making the plaque vulnerable. In the final stage, various enzymes (e.g., matrix metalloproteinases) and inflammatory cytokines are secreted by macrophages within the plaque that can lead to degradation of the fibrous cap [13]. Plaque rupture and subsequent thrombus formation can lead to blockage of blood flow to the arteries of the heart or brain, resulting in a devastating myocardial infarction or stroke, respectively **(Figure 2)** [14].

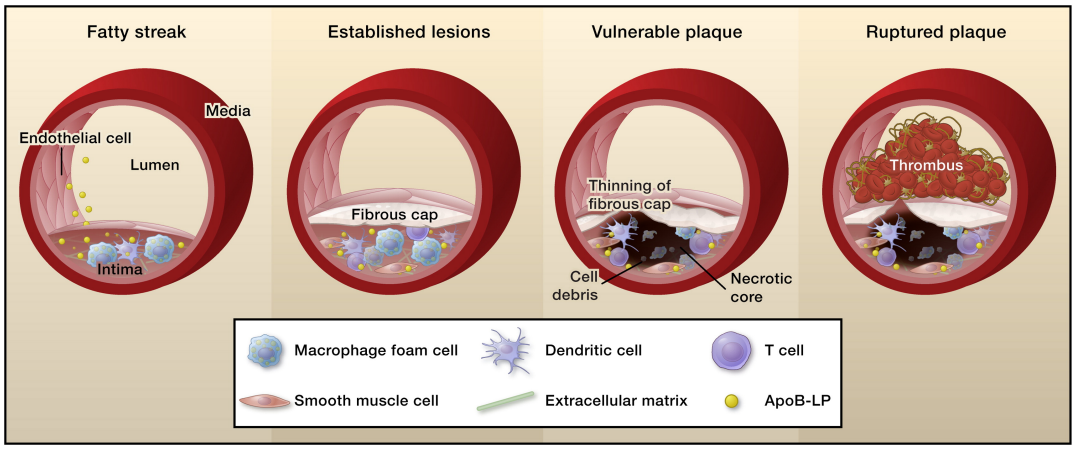

Figure 2. The progression of an atherosclerotic lesion. The accumulation of modified lipoproteins, attracts immune cells (e.g., dendritic cells and macrophages) that transmigrate to the intima. Smooth muscle cells are mobilized to form a protective fibrous cap against the lipid-filled necrotic core. Over time the thinning fibrous cap deceases stability, which may lead the atherosclerotic plaques to rupture and form a thrombus [14].

Macrophages are the most prominent cell type that drives the chronic inflammation responsible for the development of atherosclerotic plaque. Macrophages can be polarized to a

pro-inflammatory, atherogenic state (termed M1), or an anti-inflammatory, protective state (termed M2). ApoB-LPs bind to proteoglycans in the intima and are modified (e.g., oxidation and hydrolysis). These modified ApoB-LPs trigger an inflammatory response by causing cytokine and chemokine secretion. This contributes to the buildup and retention of modified lipoprotein. This inflammatory response signals macrophages to phagocytose modified lipoproteins in an uninhibited fashion, leading to the development of lipid-laden macrophage foam cells **(Figure 3)** [12, 14]. Since macrophages play a vital role in atherosclerosis development, it is important to investigate their function in the context of atherosclerosis as it is a potential therapeutic target.

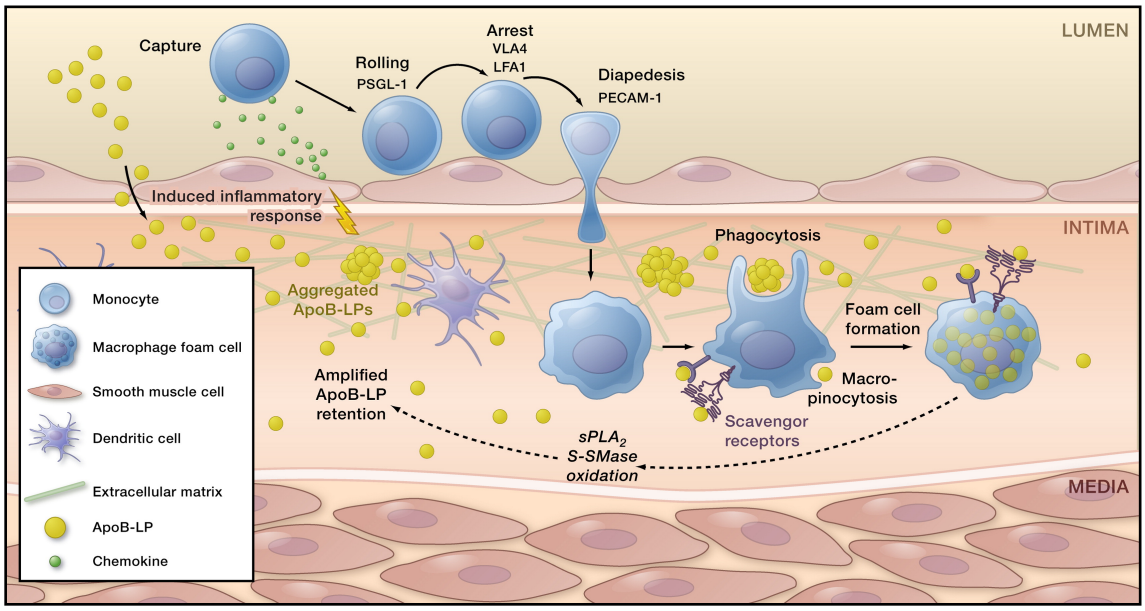

Figure 3. ApoB-Lipoprotein modification attracts macrophages and leads to foam cell formation. Lipoproteins accumulate in the intima of aortic vessel walls and are modified by oxidation or hydrolysis. These modifications trigger an inflammatory response which signals monocyte recruitment through the endothelial monolayer to the intima. The monocytes then differentiate into macrophages and phagocytose modified lipoproteins, leading to foam cell formation [14].

2. Interleukin-37 (IL-37)

Since its discovery in 2000 by *in silico* research, the Interleukin (IL)-1 family cytokine IL-37 has gained much attention due to its potent anti-inflammatory properties that broadly suppresses innate immunity [15]. Recently, the mechanisms by which IL-37 functions have been further elucidated to include both intra- and extracellular pathways involving the transcription factor Smad3 and the orphan receptor IL-1R8 (also known as SIGIRR or TIR8), respectively. IL-37 is part of the IL-1 family of cytokines, which are comprised of eleven proteins and have similar ß-barrel structures. There are five known IL-37 splice variants, designated a-e [16] (**Figure 4).** The transcripts have been found in human blood monocytes, tissue macrophages, plasma cells, neoplastic cells, synovial cells, tonsillar B cells, and in epithelial cells of the skin, kidney, and intestines. The longest isoform, IL-37b, is predominantly found in immune cells and is the most well-characterized to date [17].

There is no known mouse homolog of human IL-37, however, a landmark 2010 publication by Nold *et al.* [18] showed that transgenic mice expressing human IL-37b were protected from acute inflammation. Human IL-37 has been found to be functional in mice, paving the way for research studies using mouse models to investigate the role of IL-37 in various inflammatory diseases. Many research studies using human samples have shown that IL-37 expression was strongly associated with many inflammatory diseases, both autoimmune [19-23], and infection-related [24, 25]. Elevated plasma IL-37 levels have also been found in human patients with acute coronary syndrome [26] and atrial fibrillation [27]. Research using mouse models of pathogenic cardiovascular inflammation, including ischemia/reperfusion (I/R) injury [28, 29], myocardial infarction (MI) [30, 31], and vascular calcification [32, 33], reveal a significant benefit from IL-37 expression or treatment *in vivo*, indicating promising therapeutic

value. My thesis aims to explore the role of recombinant IL-37 and its receptor, IL-1R8, in preventing atherogenic macrophage function.

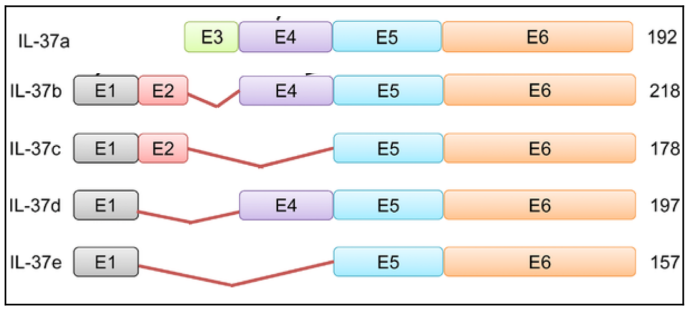

Figure 4. Human IL-37 gene structure. There are five IL-37 splice variants a-e. IL-37 isoforms a, b, and d all have exons 4, 5, and 6; the extracellular activity is located in these exons. Recombinant IL-37b is highly active (adapted from [17]).

2.1. IL-37's anti-inflammatory properties

IL-37 plays an important role in dampening innate inflammation. When endogenous IL-37 expression was downregulated in human PBMCs (peripheral blood mononuclear cells), there was an increase in production of IL-1β and other cytokines following TLR activation [18]. Transgenic mice expressing human IL-37 (Tg) show protective phenotypes in models of endotoxic shock, myocardial ischemia, colitis, and spinal injury [17, 18, 30, 31, 34]. Treating wildtype mice with recombinant IL-37 decreased inflammation in mouse models of myocardial infarction [30, 31], rheumatoid arthritis [35], and liver disease [36]. IL-37 is expressed at low levels under basal conditions, but inflammatory stimulus leads to an increase in IL-37 serum concentrations as seen in human patients with acute coronary syndrome [17, 37]. By knocking down endogenous IL-37 in primary human blood monocytes, there is an increase in TNF-α, IL-1α, IL-1β, and IL-6, supporting IL-37's anti-inflammatory properties [18, 38].

2.2. Extracellular pathway

IL-37 has been shown to act both intracellularly through the transcription factor Smad3, and extracellularly by complexing with the receptors IL-18Rα and IL-1R8 [38]. IL-37 was initially shown to prevent IL-18-induced inflammation by binding to the IL-18 binding protein

(IL-18bp) and preventing IL-18 inflammatory signaling [39]. IL-37 has a similar structure to IL-18 and binds to IL-18Rα to competitively inhibit IL-18, a pro-inflammatory cytokine [40]. IL-37 also shares significant homology with another anti-inflammatory member, IL-1 receptor antagonist (IL-1Ra), which competitively inhibits IL-1β from binding the IL-1R [41]. The extracellular function of IL-37 has been investigated in several studies. For example, treating IL-37Tg mice with neutralizing antibodies against IL-37 after LPS stimulation resulted in a reversal in IL-6, IL-1β, and TNF-α serum levels, which further supports the anti-inflammatory role of IL-37 as a classic cytokine, functioning as an extracellular mechanism [42]. Another study revealed that treating LPS stimulated macrophages with low concentrations of recombinant IL-37 (0.1-10ng/ml) significantly reduced *in vitro* cytokine production [43].

Recently, IL-37 has been found to form a tripartite complex with IL-18Rα and the orphan receptor IL-1R8 (SIGIRR) which acts to inhibit pro-inflammatory Interleukin Receptor (ILR) and Toll-like Receptor (TLR) signaling. Disruption of the tripartite complex formation by inhibiting either IL-18Rα or IL-1R8 (SIGIRR) in THP-1 macrophages or PBMCs resulted in significant reversal of the anti-inflammatory effects of IL-37 *in vitro* and *in vivo* [44], confirming the indispensable role of IL-1R8 for proper extracellular IL-37 function.

3. Interleukin 1 Receptor Family Member 8 (IL-1R8/SIGIRR):

Interleukin 1 Receptor Family Member 8 (IL-1R8) was originally discovered in 1998 and is formerly known as Single Immunoglobulin Interleukin-1 Related Receptor (SIGIRR or TIR8) [45]. IL-1R8 is an orphan receptor lacking a specific ligand and is considered a fringe member of the Interleukin Receptor (ILR) family **(Figure 5)**. Unlike the pro-inflammatory members of the ILR family, this unique receptor interferes with ILR and Toll-Like Receptor (TLR) complexing

that impairs signal transduction and negative regulation of ILR and TLR inflammatory signaling [18, 46].

IL-1R8 is highly conserved across vertebrates and there is approximately 82% homology between the protein sequences of human and mouse [47]. IL-1R8 is expressed in various tissues, including lung, liver, kidney, intestine, and lymphoid organs. It is also expressed in leukocytes, such as monocytes, dendritic cells, natural killer cells, B-cells, and T-cells [45, 48].

The structure of IL-1R8 is comprised of an extracellular Ig domain, a transmembrane domain, a cytoplasmic TIR domain, and an intracellular amino acid tail. Compared to other ILRs, which have three extracellular Ig domains, IL-1R8 has only one extracellular Ig domain. IL-1R8's intracellular TIR domains lack two conserved amino acid regions where Cys222 replaces a Ser amino acid and Leu305 replaces a Tyr amino acid [45]. These two phosphorylation sites are conserved in the other IL-1R family members, which most likely contribute to the classical function of ILR and TLR signaling. Another unique characteristic of IL-1R8 is that it has an unusually long tail containing 95 residues. These unconventional features are speculated to contribute to the negative regulation of ILR and TLR signaling [17, 38, 49].

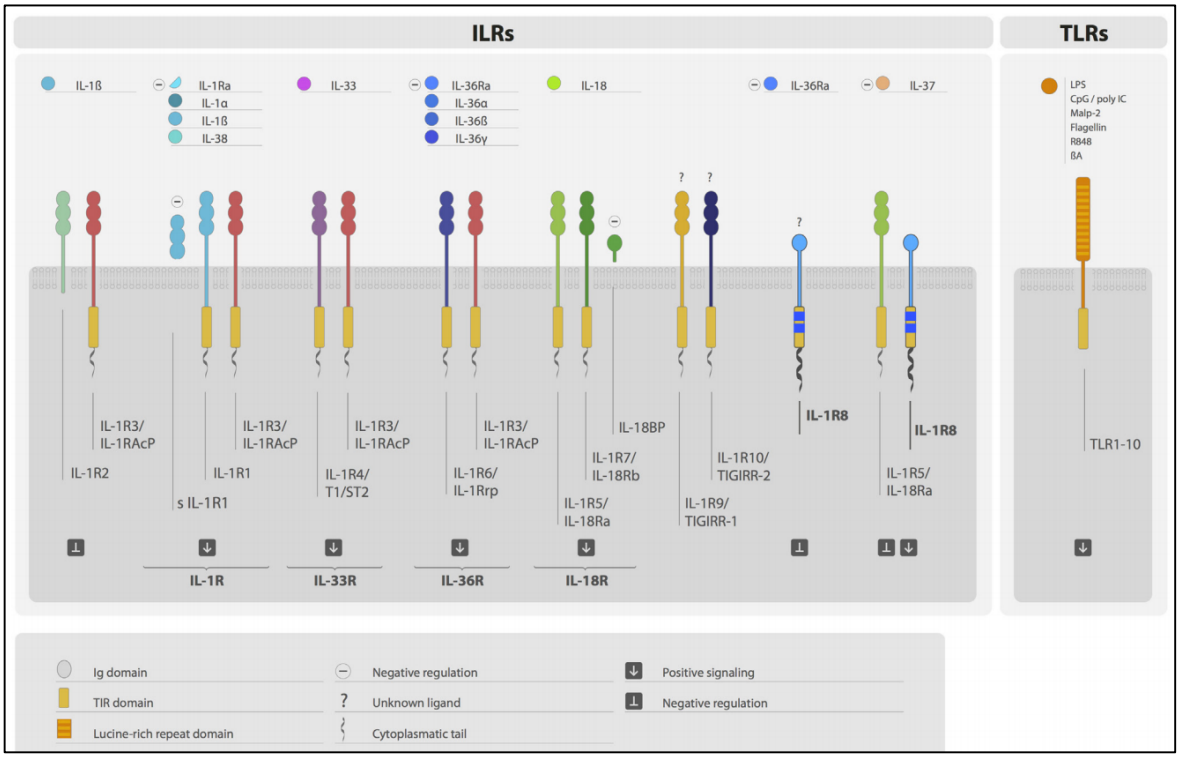

Figure 5. The Interleukin (IL)-1 Receptor and Toll-like Receptor (TLR) superfamily. Shown are the ligands, receptors, accessory proteins, and regulators involved in this IL-1R and TLR family of receptors. IL-1R8 (SIGIRR) is a fringe member of the IL-1R family and is related to the TLR family. IL-37 complexes with IL-18Rα and IL-1R8 to negatively regulate inflammation [49].

3.1. IL-37/IL-1R8's mode of action in modulating inflammation

IL-37 signals through IL-18Rα and IL-1R8 forming a tripartite complex **(Figure 6).** In particular, IL-1R8 is described as a co-receptor that is required for the anti-inflammatory function of IL-37. Investigating this tripartite complex is crucial to understanding the possible protective and anti-inflammatory function of IL-1R8 and IL-37 on macrophages in the context of atherosclerosis [38, 49]. Treatment with pro-inflammatory mediators, such as LPS, downregulates IL-1R8 by reducing SP-1-dependent promoter activation through the TLR4-p38 MAP kinase pathway [34].

The formation of the IL-37/IL-18Rα/IL-1R8 tripartite complex modulates the phosphorylation of various downstream intracellular signaling pathways. In LPS-stimulated

macrophages and dendritic cells isolated from IL-37Tg mice, the formation of the IL-37/IL-18Rα/IL-1R8 tripartite complex lead to reduced phosphorylation of TAK1, Fyn, IκBε, p65 and p105. Additionally, extracellular IL-37 signaling increased phosphorylation of the anti-inflammatory mediators Stat3, Mer, PTEN and p62 [44, 49]. Overall, this modulation of phosphorylation of key signaling proteins acts to suppress the inflammatory response overall.

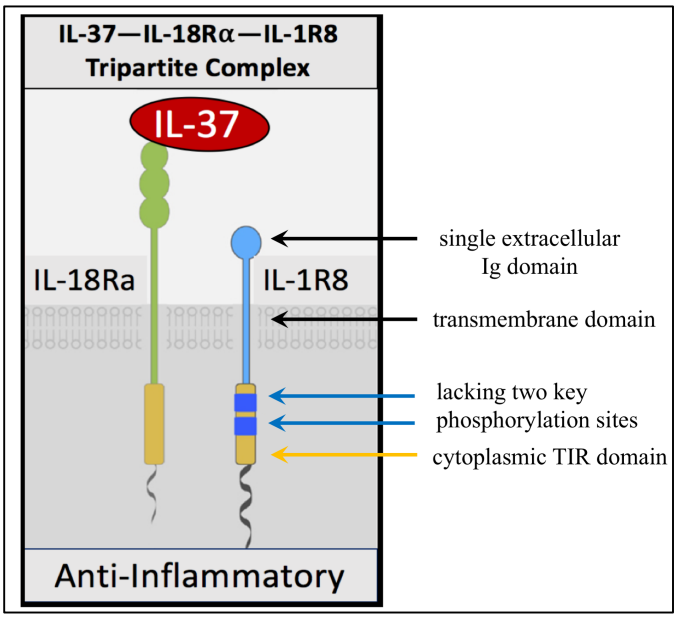

Figure 6. IL-37/IL-18Rα/IL-1R8 tripartite complex. The anti-inflammatory activity of IL-37 is achieved via formation of a membrane bound IL-37/IL-18Rα/IL-1R8 tripartite complex. IL-1R8's structure is comprised of a single extracellular Ig domain, a transmembrane domain, a cytoplasmic TIR domain, and an intracellular amino acid tail lacking two key phosphorylation sites (Adapted from [49]).

3.1.1. IL-1R8$^{-/-}$ mice and response to inflammation

IL-1R8$^{-/-}$ mouse models were developed to determine the function of IL-1R8 during *in vivo* immune responses to LPS, IL-1, and TNF stimulation. When IL-1R8$^{-/-}$ mice were injected intraperitoneally with LPS, a TLR4 activator, they exhibited an increased inflammatory response compared to wildtype mice. After the LPS endotoxin challenge, only 10% of the IL-1R8$^{-/-}$ mice survived with the remaining dying within 2 days due to severe inflammatory response compared to 70% of wildtype mice that survived. Additional pro-inflammatory mediators, including human IL-1 and TNF (isoforms not specified) were tested and although TNF did not affect the two strains differently, IL-1 resulted in a similar hypersensitive response in IL-1R8$^{-/-}$ mice. This is

further evidence that IL-1R8 plays an important role in negatively regulating inflammatory response to IL-1 and LPS *in vivo* [50].

Under *ex vivo* conditions, primary kidney epithelial cells from IL-1R8$^{-/-}$ mice were treated with the pro-inflammatory mediators, LPS or IL-1. In both cases, IL-1R8$^{-/-}$ cells had an increased NF-κB DNA binding response and prolonged activation of JNK, indicating an increase in inflammation and apoptosis, respectively. Primary splenocytes from IL-1R8$^{-/-}$ mice exhibited a similar increase in NF-κB DNA binding response and prolonged activation of JNK after LPS or IL-1 treatment, but not with TNF treatment. There was also a 2-3 fold increase in the rate of cell proliferation after LPS treatment in IL-1R8$^{-/-}$ primary mice splenocytes supporting IL-1R8's negative regulation of inflammatory response [50].

To determine the dependence of IL-37 on IL-1R8 for its anti-inflammatory function, IL-37Tg mice were crossed with IL-1R8$^{-/-}$ mice. After the IL-37Tg mice were intraperitoneally injected with LPS, pro-inflammatory cytokine IL-6 and inflammatory chemokine MIP-2 was lowered 53% and 76%, respectively. IL-1R8$^{-/-}$ and wildtype mice resulted in similar cytokine fold changes. In IL-37Tg X IL-1R8$^{-/-}$ mice, the reduced inflammation observed in IL-37Tg mice was abrogated. The gene expression of IL-6 and MIP-2 in the lungs was 64% and 60% less effective, respectively, in IL-37Tg X IL-1R8$^{-/-}$ mice than in IL-37Tg mice, which supports IL-37 and IL-1R8's protective role in attenuating inflammation [18, 38].

3.2. Glycosylation properties of IL-1R8

One proposed method of IL-1R8 regulation is asparagine N-linked, and serine or threonine O-linked, protein glycosylation. With human and mouse IL-1R8 proteins being 82% identical, the human IL-1R8 protein has five potential N-glycosylation sites in the extracellular region of IL-1R8, whereas mouse IL-1R8 has four potential N- and O-glycosylation sites on the

asparagine amino acids **(Figure 7)** [51]. IL-1R8 protein molecular weight ranges from 44kDa (unglycosylated) to 90kDa (glycosylated). Glycosylation of IL-1R8 has been investigated in human epithelium colon cancer cells and tissues, human VACO colon cancer cells, HeLa cells, mouse endothelium, COS-7 kidney cells, renal tubular epithelial cells, and spleen monocytes [45, 48, 51]. IL-1R8 protein detected by Western blot analysis reveals heavy glycosylation, a post-translational modification that is suggested to inhibit the negative regulation of IL-1R8. When HeLa cells were transfected with mutant IL-1R8/SIGIRR cDNA, the IL-1R8 glycosylation was reduced from 90kDa to around 55kDa [51]. Treatment with the glycosidase PNGase F also served to confirm N-linked glycosylation of IL-1R8 in human colonic epithelial cells, COS-7 kidney cells, renal tubular epithelial cells, and spleen monocytes [45, 48, 51].

```
Human   1 MPGVCDRAPDFLSPSEDQVLRPALGSSVALNCTAWVVSGPHCSLPSVQWLKDGLPLGIGG
Mouse   1 MAGVCDMAPNFLSPSEDQALGLALGREVALNCTAWVFSRPQCPQPSVQWLKDGLALGNGS
            * **** ** ******** *  ***  ********* * * *  ********** ** *
Human  61 HYSLHEYSWVKANLSEVLVSSVLGVNVTSTEVYGAFTCSIQNISFSSFTLQRAGPTSHVA
Mouse  61 HFSLHEDFWVSANFSEI-VSSVLVLNLTNAEDYGTFTCSVWNVSSHSFTLWRAGPAGHVA
            * ****  ** ** **  *****  * *  * ** ****  * *  **** ****  ***
```

Figure 7. IL-1R8 (SIGIRR/TIR8) is N-linked glycosylated in human and mouse. This is a partial cDNA sequence of mouse and human IL-1R8 where the underlined amino acids show conserved N-linked glycosylated motifs [51]. * represents conserved amino acids.

N-linked glycosylation is a complex and multistep process that begins in the endoplasmic reticulum (ER) where high mannose modification occurs, involving the addition of two N-acetylglucosamines with many mannose residues to the nascent protein, which is then transported to the Golgi apparatus for additional processing **(Figure 8)**. It is hypothesized that post-translational glycosylation regulates TLR's influence on surface representation, protein trafficking, and pattern recognition [52]. Dysregulation of TLR glycosylation can lead to uncontrolled inflammation, irregular intracellular trafficking and protein folding, and the promotion of cancer. Zhao *et al.* show that both complex glycan modification and cell surface

expression was required for IL-1R8 function [48, 51, 53]. Understanding the role and extent of IL-1R8 glycosylation in bone marrow derived macrophages (BMDM) and RAW 264.7 macrophages may provide insight into IL-1R8's role in inflammation in the context of atherosclerosis.

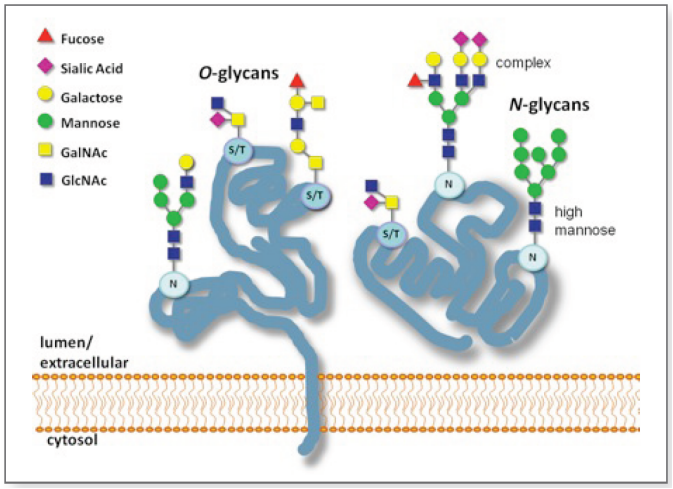

Figure 8. Common glycosylation patterns for secreted and cell-surface glycoproteins. N-and O-glycosylation is a main post-translational modification in eukaryotic cells. N-glycosylation occurs at the asparagine amino acid and O-glycosylation occurs at the serine and threonine amino acid [54].

4. Therapeutic Potential for IL-37/IL-1R8 in inflammatory diseases

One of the purposes of the immune system is to regulate and protect against disease, but a dysregulated immune response can lead to inappropriate chronic inflammation, and subsequent tissue damage. The IL-37/IL-18Rα/IL-1R8 tripartite complex is a potential therapeutic avenue to protect against inflammatory diseases, including infection (e.g., *Mycobacterium tuberculosis*), autoimmune disease (e.g., rheumatoid arthritis), kidney disease (e.g., lupus nephritis and post-ischemic acute renal failure), neuronal inflammation (e.g., Alzheimer's disease), intestinal inflammation and cancer, and chronic cardiovascular inflammation (e.g., atherosclerosis) [49].

IL-37 has been shown to decrease inflammation in human and mouse primary macrophages and cell lines (e.g., THP-1 and RAW 264.7 Macrophages) [18]. Interestingly, IL-37Tg mice were better protected than wildtype mice from lipopolysaccharide (LPS) endotoxic shock [18]. In an experimental dextran sulfate sodium (DSS)-induced colitis mouse model, IL-

37Tg mice compared to control mice decreased clinical colitis disease scores by 50% and reduced pro-inflammatory cytokines, IL-1ß and TNFα [55]. Also, in an *in vivo* Concanavalin A (ConA) induced hepatitis model, IL-37Tg mice stimulated with ConA significantly reduced IL-1α, IL-6, IL-5, IL-9 cytokine production compared to control mice [36]. These *in vivo* studies support an anti-inflammatory and protective role of IL-37 in various inflammatory disease settings.

A recent study has shown that IL-37 is elevated in peripheral blood mononuclear cells from acute myocardial infarction patients [36]. In both atherosclerosis and MI, the accumulation of pro-inflammatory cytokines leads to vascular inflammation which causes accelerated necrosis, apoptosis, and endothelial dysfunction [14]. Downstream effects showed that with IL-37 treatment, NF-κB was downregulated which would decrease apoptosis and cardiac injury. This was protective in cases of atherosclerosis and MI related heart failure [31]. The IL-37/IL-18Rα/IL-1R8 tripartite complex has been shown to be indispensable for IL-37 to function extracellularly. Since anti-inflammatory therapies using IL-37 will most likely involve systemic treatment with recombinant protein, understanding and potentially controlling the regulation of IL-1R8 expression for this purpose is important. Acting together, IL-37 and IL-1R8 are part of a complex with potential therapeutic value in reducing the chronic inflammation that drives atherosclerosis development.

CHAPTER 2: MATERIALS AND METHODS

1. Media, Buffers, and Solutions

1.1. Media, Buffers, and Solutions for Cell Culture

Media, buffers, and solutions were prepared under sterile conditions. Media was purchased from Gibco by Life Technologies. Dulbecco's modified eagle medium (DMEM) was used to culture L929, RAW 264.7 mouse macrophages. Fetal Bovine Serum (FBS) was heat inactivated 56 °C for 1 hour before use.

Table 1: Medium composition for cell culture

Cells	Name	Composition
All	Freezing Medium	90% FBS 10% Dimethylsulfoxide (DMSO)
Bone Marrow Derived Macrophages	Differentiating Medium (complete)	DMEM/ F12 + L-Glutamine 10% FBS 20% L929 conditioning medium 1% Penicillin/Streptomycin Filter with 0.22um filter unit
Bone Marrow Derived Macrophages	Experimental Medium	DMEM/ F12 + L-Glutamine 10% FBS 1% Penicillin/Streptomycin Filter with 0.22um filter unit
L929 (M-CSF Supernatant)	Growth Medium	DMEM + L-Glutamine, Na^{2+} Pyruvate 10% FBS 1% Penicillin/Streptomycin 1% 1M HEPES
RAW 264.7 Mouse Macrophages	Growth Medium	DMEM + L-Glutamine, Na^{2+} Pyruvate 10% FBS 1% Penicillin/Streptomycin Filter with 0.22um filter unit

1.2. Buffers and Solutions

Table 2: Buffer and solution composition

PBS	150mM NaCl 120mM KCl 10nM Na2HPO4/KH2PO4 pH 7.4
PBS- Tween	PBS 0.1% Tween
RIPA buffer	50mM Tris-HCl

	1% Triton X-100 0.5% Na deoxycholate 0.1% SDS 150mM NaCl 2mM EDTA H_2O
SDS-Loading buffer	0.1 M Tris-HCl pH 6.8 0.7% SDS 33% glycerol 0.01% bromophenol blue 8% b-mercaptoethanol
TAE	40 mM Tris-acetate 1 mM EDTA pH 8.3
LB (Luria- Bertani) medium	10g/L Bacto-tryptone 5g/L yeast extract 10g/L NaCl

2. Cell lines

Table 3: Cell lines for transfection

Cell Line	Description	ATCC Number
L929	Organism: *Mus musculus*, mouse Tissue: subcutaneous connective tissue; areolar and adipose Morphology: fibroblast	CCL-1
RAW 264.7 Macrophages	Organism: *Mus musculus*, mouse Tissue: Abelson mouse leukemia virus-induced tumor; ascites Morphology: monocytes/macrophages	TIB-71

3. Mouse Strain

Wildtype C57BL/6 mice originally purchased from Jackson Laboratories were housed in the University of Hawaii John A. Burns School of Medicine Vivarium animal facility. Male 8-12 week old wildtype mice were used for all *in vitro* experiments. The use of only the male sex served as a control, as female mice may have a different response. Animal protocols were approved by the University of Hawaii Institutional Animal Care and Use Committee.

4. Antibodies

Table 4. Antibodies for Western blotting

Target	Name	Company	Isotope	Application	Dilution
IL-1R8/ SIGIRR	A-4	Santa Cruz Biotechnology, Inc.	1° Mouse monoclonal	Western blot	1:500
IL-1R8/SIGIRR	C-12	Santa Cruz Biotechnology, Inc.	1°Goat polyclonal	Western blot	1:500
GAPDH	60004-1-Ig	Protein Tech Group	1° Mouse monoclonal	Western blot	1:1000
MYC	71010	Cell Signaling Technology	1° Rabbit monoclonal	Western Blot	1:1000
Donkey anti-mouse	IR Dye 680RD	Li-Cor, 926-32210	2°	Western blot	1:10,000
Donkey anti-goat	IR Dye 800CW	Li-Cor., 926-68074	2°	Western blot	1:10,000

5. Plasmids

Table 5: Plasmids for transfection

Plasmid	Cat. No.	Description
GFP		pcDNA3.1-CMV-GFP
IL-1R8/SIGIRR	MR206419 NM_023059	Sigirr (C-terminal Myc- DDK tagged) Mouse cDNA ORF Clone, pCMV6 entry 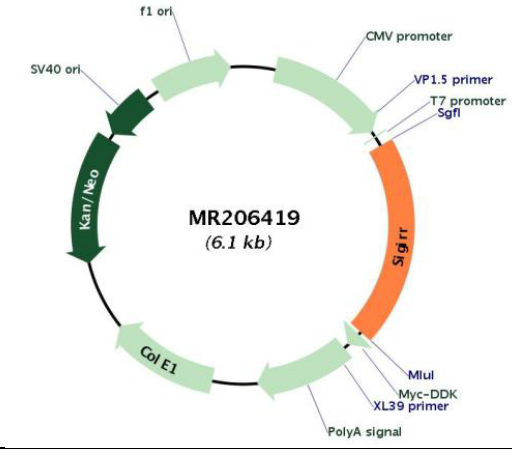

6. siRNA reagents

Table 6: siRNA for knockdown transfection

Name	Company
Scrambled siRNA Smart Pool- IL-1R8	Dharmacon
siRNA Smart Pool- IL-1R8	Dharmacon
X-tremeGENE siRNA Transfection Reagent	Roche

7. Primers

Table 7: List of primers for PCR, RT-qPCR, Western blotting

Gene	Forward Sequence (5'-3')	Reverse Sequence (5'-3')
Gapdh	GGCAAATTCAACGGCACAGT	CGCTCCTGGAAGATGGTGAT
IL-1R8 (version 1)	TCCATGAGGACTTCTGGGTCAG	AGAACAGGTGAAGGTTCCATAGTCC
IL-1R8 (version 2)	TCCATGAGGACTTCTGGGTCAG	TCAGCCGACACTTAACATAGAGCA
IL-1β	TCCAGGATGAGGACATGAGCAC	GAACGTCACACACCAGCAGGTTA
IL-6	TCTTGGGACTGATGCTGGTGACAAC	TGCCATTGCACAACTCTTTTCTCATTT
iNOS	TGCATGGACCAGTATAAGCGAAG	GCTTCTGGTCGATGTCATGAGCAA
TNFα	CTGTAGCCCACGTCGTAGC	GGTTGTCTTTGAGATCCATGC
MCP1/ CCL2	TCACTGAAGCCAGCTCTCTCT	GTGGGGCGTTAACTGCAT
ABCA1	CCCAGAGCAAAAAGCGACTC	GGTCATCATCACTTTGGTCCTTG
ABCG1	CAAGACCCTTTTGAAAGGGATCTC	GCCAGAATATTCATGAGTGTGGAC
PPARγ	GCAGCTACTGCATGTGATCAAGA	GTCAGCGGGTGGGACTTTC
MMP2	GTAAAGTATGGGAACGCTGATGGC	CATGGTAAACAAGGCTTCATGGGG
MMP3	TGGAACTCCCACAGCATCCC	GCGCCAAAAGTGCCTGTCTTT

8. Cell Culture Methods

All cell culture methods were conducted in biosafety hoods to maintain sterility. Cells were maintained at 37 °C in a humidified incubator with 5% CO_2. Cell culture medium was pre-warmed to 37 °C before use. Cell culture materials included: 15ml and 50ml Falcon tubes, cell scraper, cell lifter, T-75 flasks (Fisher).

8.1. Bone marrow derived macrophage (BMDM) cell isolation, *in vitro* cell culture

Male wild type C57BL/6 mice, 8-12 weeks old, were euthanized by CO_2 asphyxiation and sprayed with 70% EtOH for disinfection. The femur and tibia bones were isolated under the sterile conditions. The bones were flushed with 20-25ml of ice cold sterile PBS using a 25-gauge needle into a 50mL Falcon tube and kept on ice. The isolated bone marrow cells were resuspended with a 10ml pipette, passed through a 40μm cell strainer into a new 50ml Falcon tube, and centrifuged at 1300 rpm for 5 minutes. The supernatant was aspirated and the cells

were resuspended in BMDM complete differentiation medium (DMEM/F12 supplemented with 10% fetal bovine serum, 20% L929-conditioned medium, and 1% penicillin/streptomycin). Live cells were counted using a dilution of 1:3 or 1:5 in 0.4% trypan blue solution. 10µl of diluted cells were added to each side of a hemacytometer and cells in four separate quadrants were counted and averaged.

The bone marrow stem cells were differentiated into macrophages by plating 10-15x10^6 cells per 15-cm^2 tissue culture plate (Corning) in 25mL of BMDM complete differentiation medium. On days 3 and 5, an additional 10mL of differentiating medium were added to each plate. On day 7, the differentiating medium was aspirated and the BMDM were detached with 4ml Cell Stripper (Gibco) per plate for 5-10 minutes at 37 °C. Next, the differentiated BMDM were gently removed using a cell lifter, washed with 5ml of PBS, and centrifuged at 1300rpm for 5 minutes. The cells were then counted and replated into 6-well plates at 3-3.5x10^6 cells per well for *in vitro* experiments. BMDM were stimulated with 10-25ng/ml IFNγ, 10ng/ml-100ng/ml LPS or 10ng/ml IL-4 for 1-24 hours.

L929 conditioned medium was produced by plating 4.7x10^5 L929 cells per 75 cm^2 flask in 50ml of medium (DMEM, 10% FBS heat inactivated, 1% HEPES, and 1% Pen/Strep). The L929 cells were incubated for 7 days, at which point the medium was collected and sterile filtered with 0.22µm filter unit. Then the supernatant was aliquoted into 50ml falcon tubes and stored at -20 °C (short term) or -80 °C (long term).

8.2. RAW 264.7 Macrophages, *in vitro* cell culture

Cryopreserved RAW 264.7 Macrophages were removed from the -150°C freezer and thawed in a 37°C water bath until almost all the ice was thawed (30-90seconds). The cryovials were sprayed with 70% EtOH before putting in biosafety hood, and 1ml of warm media was

added to each vial. The cell suspension was added to 5 ml of growth media in a 15ml falcon and centrifuged at 1300 rpm for 5 minutes. The supernatant was aspirated and the cells were resupsended in 15 ml of growth media and transferred to a T-75 cell culture flask.

The RAW 264.7 macrophages were cultured in T-75 flasks. Cells were split no more than 1:4 when they reached 70-80% confluency. The cells were washed with PBS and detached with 1ml of 0.25% Trypsin-0.53mM EDTA and placed in the 37°C incubator for 3-5 minutes. Then 4ml of cell medium was added to inhibit the Trypsin. The cells were resuspended and mixed thoroughly to prevent clumps before splitting into new T75 flasks in a total volume of 15ml each. For experiments, the cells were counted and replated into 6-well plates at 2.5-3.5x10^5 cells per well for *in vitro* experiments.

For freezing RAW 264.7 macrophages, once they reached 70-80% confluency the cells were harvested, counted, and centrifuged at 1300rpm for 5minutes. The supernatant was aspirated and the cells were quickly resuspended with freezing medium (90% FBS, 10% DMSO at a concentration of 1x10^6 cells/ml. 1ml of cells was added to each cryovial and quickly transferred to an isopropanol pot and kept at -80°C for 24 hours. The cryovials were then transferred to the -150 °C for long-term storage.

9. <u>Transfection of RAW 264.7 Macrophages and BMDM with GFP and IL-1R8</u>

Once the cells reached 70%-80% confluency for RAW 264.7 cells and after 7 days of differentiation for BMDM, they were split into appropriate plates for transfection. Optimal conditions for a 24-well plate format was 1μg DNA: 2μl Lipofecatmine 2000, with 0.8 x 10^5 cells and 500μl media per well. Optimal conditions for a 6 well plate was 4μg DNA: 8μl Lipofectamine 2000, with 3-3.5x10^5 cells/well for RAW 264.7 Macrophages and 3-4x10^6

cells/well for BMDM with 2ml media per well. The manufacturer's protocol for Lipofectamine 2000 was followed for transfection experiments (Life Technologies).

10. IL-1R8 siRNA Transfection of RAW 264.7 Macrophages and BMDM

In a 6 well plate, 3-3.5x10^5 RAW 264.7 Macrophages/well and 3-3.5x10^6 BMDM cells/well were plated in a total of 2ml media per well. The test conditions consisted of 400µl of combined 50nM or 100nM Scrambled or IL-1R8 siRNA, 10µl of Roche Xtreme Gene siRNA transfection reagent, and OptiMem antibiotic free medium for 24 or 48hours. See Dharmacon Smart Gene Pool and Roche Xtreme siRNA transfection reagent protocol.

11. Molecular Biology Methods

11.1 RNA Isolation and cDNA Preparation

After the BMDM were harvested and stabilized with RNA Later, 500µl of TRIzol was added to the frozen cell pellet in a 1.5mL tube. The samples were vortexed until the pellets dissolved and then 100µl of chloroform was added. The samples were inverted 5 to 10 times. Once properly mixed, the samples were centrifuged for 15 minutes at 12400 rpm at 4°C. The aqueous phase was carefully transferred into a new tube and 1X volume of 70% ethanol was added. The samples were gently inverted and added to the Qiagen RNeasy purification column and centrifuged for 15 seconds at 10000rpm. Then, 80µl of DNA digest master mix was added (70µl H_2O and 10µl DNase) and incubated for 15 minutes at RT. For the first wash step, 700µl of RW1 buffer was added to each column and samples were centrifuged at 10,000 rpm for 15 seconds, then discarded. Next, 500µl of RPE buffer was added to each column and samples were centrifuged at 10,000rpm for 15 seconds, then discarded, followed by a second wash step with an additional 500µl of RPE buffer. The samples were then centrifuged for an additional 2 minutes at 10000rpm. In the final elution step, 30µl of RNase free H_20 was warmed at 55°C and added to

the columns, which were put into RNase free 1.5ml microcentrifuge tubes, and allowed to incubate for 1-5 minutes. Tubes were centrifuged at 10,000 rpm for 1 minute, and the eluted RNA was then kept on ice. A NanoDrop spectrophotometer was used to measure the RNA concentration and quality. If not used immediately to make cDNA, the RNA was stored at -80°C.

Using a qScript cDNA synthesis kit (Quanta Biosciences), 1µg of RNA per sample was transcribed into cDNA. In a total volume of 15µl, the appropriate amount of H2O was added to the 1µg of RNA. Then, 4µl of 5x reaction buffer and 1µl of reverse transcriptase enzyme per sample were added for a total of 20µl per sample. The cDNA samples were run on the following program: After cDNA synthesis, 80 µl of RNase free H_2O per sample was added to make a total of 100µl cDNA at a concentration of 10ng/µl. The cDNA qScript assay was run on a Peltier Thermal Cycler 225 PCR System (Stage 1: 25 °C for 5 minutes; Stage 2: 42 °C for 30 minutes, Stage 3: 85.0 °C for 5 minutes, Stage 4: 10.0 °C forever).

11.2. Polymerase Chain Reaction (PCR)

For a PCR assay, 7µl of H_2O was added to 1µl of combined 10nM forward and reverse primer mix and vortexed thoroughly. Then, 10µl of 2X Go Taq green master mix was added to the H_2O and primer master mix. The PCR components were gently mixed and then 2µl of cDNA was added for a total of 20µl per sample. PCR assays were run on a Peltier Thermal Cycler 225 PCR System (Stage 1: 95 °C for 5 minutes; Stage 2: 95 °C for 30 seconds, Stage 3: 57.0 °C for 30 seconds, Stage 4: 72.0 °C for 1 minute, 35 times).

After the PCR program was completed, a 1-1.5% agarose gel was made with 1X TAE buffer. 1µl of Sybr Safe stain was added for every 10ml of agarose gel. Once the agarose gel hardened, 1X TAE was poured into the chamber and 10µl of ladder was added in the first lane.

Then, the samples were loaded. For a 50ml gel, the program ran at 125 volts for 30 minutes. For a 100ml gel, the program ran at 150-200 volts for 45-60 minutes. After the DNA bands were completely separated, the agarose gel was imaged on the Typhoon scanner.

11.3. Reverse transcriptase quantitative PCR (RT-qPCR)

For RT-qPCR, 4 µl cDNA was added to each well of a 94-well plate, followed by a master mix consisting of 1µl of combined forward and reverse primer (10µM) and 13.5µl of RNase-free H20. Then, 18.5 µl of SYBR Green 2X master mix with ROX was added per well in a 96-well plate and pipetted up and down to mix. A clear adhesive film was added and the 96-well plate was centrifuged for 2 minutes at 4°C, 2200 rcf. Then, 10µl of each sample was pipetted in triplicate into a 384-well qPCR plate. GAPDH was used as a reference gene to determine expression levels of genes of interest. RT-qPCR assays for Aims I and II were run on an Applied Biosystems 7900 HT Fast Real Time PCR System (Stage 1: 95 °C for 15 minutes; Stage 2 (40 cycles): 94 °C for 30seconds, 57.0 °C for 30 seconds, 72.0 °C for 30 seconds; Stage 3: 95.0 °C for 15 seconds, 57.0 °C for 15 seconds, 95.0 °C for 15 seconds). Experiments performed for Aims II and III were run on an Applied Biosystems Quant Studio 12k Flex (Stage 1: 95.0 °C for 10minutes, Stage 2 (40cycles): 95.0 °C for 15 seconds, 57.0 °C for 30 seconds, 72.0 °C for 30 seconds, and Stage 3: 95.0 °C for 15 seconds, 57.0 °C for 1 minute).

11.4. Western blot

RIPA lysis buffer was supplemented with protease and phosphatase inhibitor cocktails at 1:100 (Thermo Fischer) and was used for all lysate sample preparation. Cells were gently washed with PBS and all liquid was aspirated before 125µl of lysis buffer was added to each sample. The 6-well plates were then incubated on ice for 15 minutes. A cell scraper was used to collect lysates, which were pipetted into 1.5ml microcentrifuge tubes. The lysates were then

sonicated at a power level of 2.5 for 10 pulses using a probe sonicator (Thermo Fisher) and centrifuged at 400 x g for 5 minutes at 4°C to pellet debris. The lysates were then transferred to a new tube and the cell debris pellets were discarded. The protein concentrations of the cell lysates were determined with the Pierce Bicinchoninic Acid Assay (BCA) kit (ThermoFisher) using a 1:10 dilution of the samples. Undiluted samples were stored at -80°C until used for Western blots.

Precast 4-12% NuPAGE Bis-Tris Mini (12-well) or Midi (20-well) gels were used for protein electrophoresis. 10-20µg of protein plus RIPA lysis buffer up to 12 µl along with 4 µl of 4x SDS Laemmli-loading buffer per sample were heated at 95 °C for 5 minutes. After cooling to RT, samples were loaded onto a precast 4-12% NuPAGE Bis-Tris Mini (12-well) or Midi (20-well) gel. The gel was run in 1X NuPAGE SDS Running Buffer (Invitrogen) at 150-200 V for 40-60 minutes.

After the blue loading dye reached the bottom of the 4-12% NuPAGE Bis-Tris gel, the cassette was opened and the gel was then used for transfer to a PVDF-FL (Immobilon) membrane. The membrane was cut to the appropriate size and activated in 100% methanol for 15 seconds. 1X Efficient™ Western Transfer Buffer (G-Biosciences® #786-019) with 20% methanol was used to prepare the gel and membrane for transfer. Four sheets of filter paper were equilibrated in transfer buffer. The gel and membrane were sandwiched between two sheets of soaked filter paper on each side and packaged tightly within a transfer cassette, which was placed in the transfer chamber with transfer buffer to the fill line. The transfer chamber containing an ice pack and stir rod was packed in ice on a stir plate to ensure that the transfer buffer remained at a cool temperature and was run at 100 volts for 1 hour.

The membrane was then blocked in LI-COR blocking buffer for 1 hour at room

temperature. Then the blot was incubated with primary antibodies, C-12 IL-1R8 (SIGIRR) or A-4 IL-1R8 (SIGIRR) (both Santa Cruz Biotechnology, 1:500) to detect SIGIRR, and GAPDH (Protein Tech, 1: 1,000) as loading control. Primary antibodies were diluted in blocking buffer and membranes were incubated on a rocker over night at 4°C. The membranes were washed with 0.1% PBS-Tween three times for 5 minutes each. The membrane was then incubated with the appropriate Licor near infrared secondary antibodies (IR-680, IR-800, both 1:10,000). The membrane was then washed three times for 5 minutes each in 0.1% PBS-Tween and the membrane was stored in PBS. The final Western blot was imaged on a Licor Odyssey infrared scanner and the images were analyzed using the Licor Image Studio software (Licor Biosciences).

11.5. Bacterial Transformation: IL-1R8 in pCMV6-entry vector

Plasmid DNA (pcDNA3.1-CMV-GFP and pCMV6-Myc-DDK-tagged-SIGIRR from Origene Product MR206419) was transformed into competent *E. Coli* (Invitrogen). 2µl of DNA was added to 50µl of competent cells on ice. The tubes were gently mixed and left on ice for 30 minutes. The tubes were then heat shocked in a 42°C water bath for 30 seconds, and then placed back on ice for 2 minutes. Next, 500 µl of LB media without antibiotics was added to each vial of bacteria and the cells were allowed to recover for 1 hour at 37°C in a shaker. The transformed bacteria were then plated on agar plates containing the appropriate antibiotic. The pCMV-SIGIRR-transformed bacteria were plated on Kanamycin-containing agar (25µg/ml) while the pcDNA 3.1-GFP-transformed bacteria were plated on Ampicillin agar plates (50µg/ml). Finally, the plates were incubated overnight at 37°C to allow colonies to grow.

Glycerol stocks of transformed bacteria were also used. A 10µl pipette tip was used to collect a bacterial sample and was added to 250ml of LB broth with appropriate antibiotic and incubated at 37°C on a shaker overnight.

Bacteria were pelleted and plasmid DNA was purified with the Pure Yield Plasmid Maxiprep System (Promega) using vacuum filtration according to the company's protocol. After the DNA concentration was measured using a NanoDrop spectrophotometer the plasmid DNA was stored at -20 °C.

11.6. In-Gel band identification

The polyacrylamide gel electrophoresis protocol in Section 11.2 was modified with the following specifications. After the concentration of protein was determined using a BCA assay, the samples were digested with PNGase F glycosidase. 15µg of protein was combined with 1 µl of glycoprotein denaturation buffer (10X), and H20 in a total of 10µl, which was incubated for 10 minutes at 100°C. Then, 2µl Glycobuffer 2, 1µl 10% NP-40, and 1µl PNGase F were added and the samples were incubated for 1 hour at 37°C. The samples were then reduced with 50nM DTT for 30 minutes at 65 °C, followed by alkylation with 10mM iodoacetamide at room temperature for 1 hour in the dark. Finally, freshly made loading dye (6X) was added and the samples were run on SDS page at a power of 150V for 60 minutes (See Section 11.2, New England Lab protocol, and Protech Cysteine Alkylation Before SDS-PAGE Protocol).

After the blue loading dye reached the bottom of the gel, the precast gel case was opened. The gel was washed in mH_2O for 10 minutes for a total of 3 times on a rocker at room temperature. The H_2O was discarded. 20ml of stain solution was added to cover the gel, which was incubated with agitation on a rocker for 5-10 minutes at room temperature until the protein stained blue. The stain solution was poured out into a waste bottle. About 15ml of destaining

solution (50% MeOH, 10% HoAC, 40% H_2O) was added to the gel and incubated on rocker for 10 minutes, followed by a lower concentration destaining solution (5% MeOH, 7.5% HoAC, 87.5% H_2O) overnight with agitation at room temperature. The gel was monitored every hour and the solution was changed out when saturated with blue stain. The gel was stored in 7% HoAC solution in the dark at 4°C until imaged.

Before the band was excised, a photograph of a gel band was taken for records. Direct contact with the gel was avoided. Blank gel space was minimized in a gel sample to improve digestion efficiency and peptide recovery. The gel band was placed in a sterile 1.5 ml microcentrifuge tube and labeled carefully. The height of each gel slice (vertical dimension) was less than 2.5 mm (Protech protocol).

12. <u>Statistical Analysis</u>

For *in vitro* experiments, at least 3 biological replicates were analyzed for each assay unless otherwise indicated. cDNA was analyzed for transcript expression with RT- qPCR analysis. Ct values were first normalized to GAPDH for each sample, and then expressed as the average fold change relative to GFP controls for each treatment, with error bars representing the SEM. For Western blot analysis, Image Studio was used to quantify the protein signal. First, the bands were selected with an equivalent square area, normalized to its respective GAPDH protein band, and then adjusted to the control treatment signal.

The Student's T-test was used to compare differences between control, LPS, IFNγ, TNFα, and IL-37 treatment groups with significance set at $p<0.05$. The p-values for all experiments was calculated using Prism (*$p<0.05$, **$p<0.001$, and *** $p<0.0001$).

CHAPTER 3: RESULTS

Preliminary Data: Determine the effect of recombinant IL-37 in macrophages.

With the hypothesis that IL-37 has potent anti-inflammatory properties in macrophages based on many studies that showed IL-37 negatively regulating inflammation, initial studies were conducted to determine the effects of recombinant human IL-37 protein on mouse primary bone marrow derived macrophages (BMDM). To do so, BMDM were co-treated with 25ng/ml IFNγ or 20ng/ml LPS and 1, 10, and 100ng/ml recombinant IL-37 for 6 hours. Transcript levels for inflammatory genes, (IL-6, IL-1b, iNOS, TNFα, MCP1/CCL2, CCL4), were analyzed with PCR and RT-qPCR.

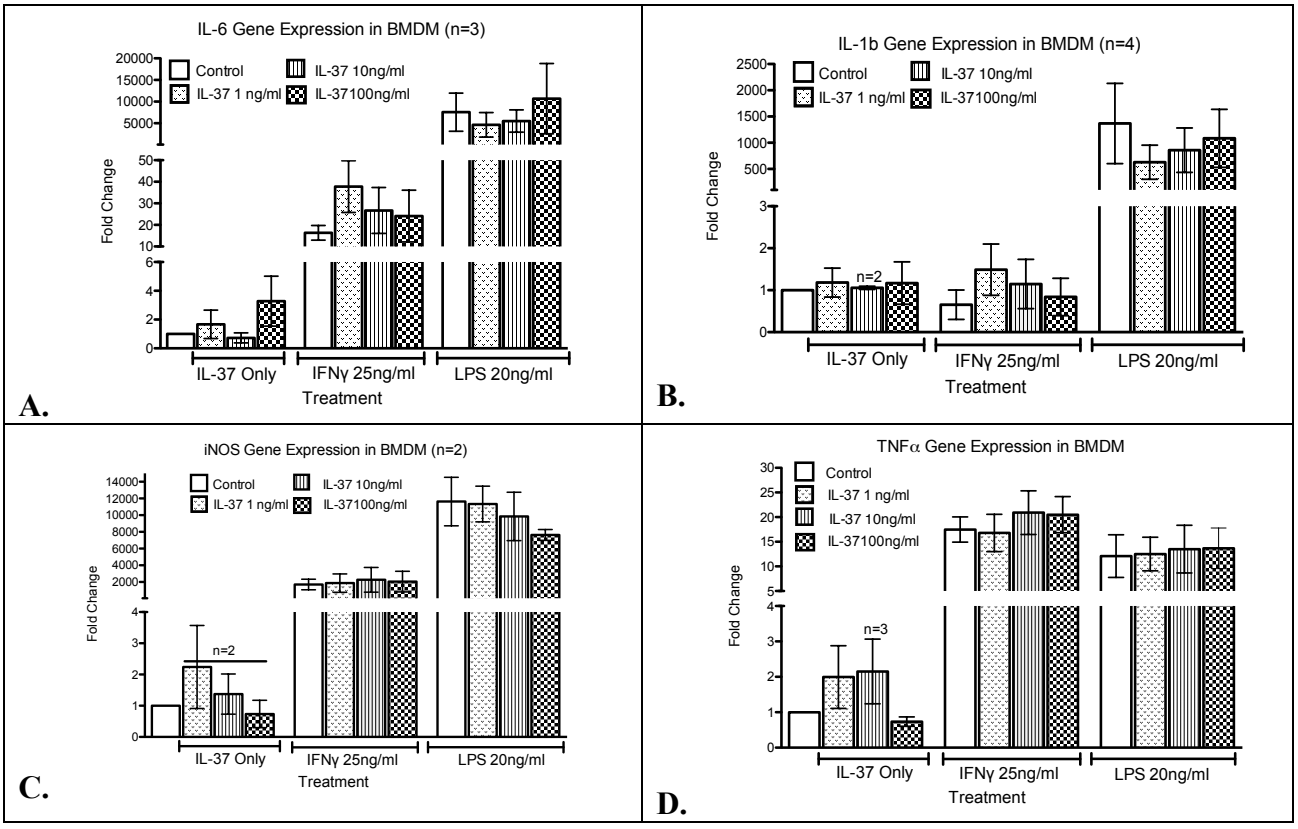

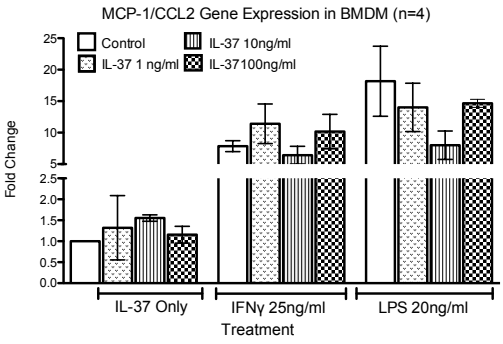

E.

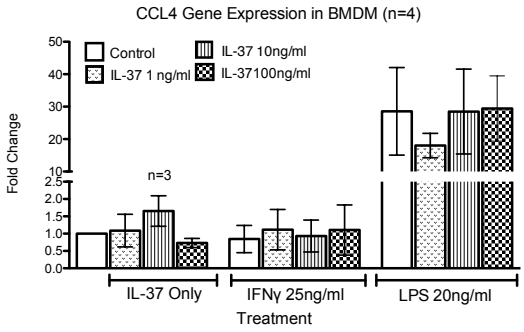

F.

Figure 9. Recombinant IL-37 protein co-treatment with LPS had no significant impact on pro-inflammatory gene expression. (A-F) With BMDM, there was no significant reduction of inflammatory IL-6, IL-1b, iNOS, TNFα, MCP1/CCL2, and CCL4 gene expression with 1, 10, or 100 ng/ml IL-37 and LPS for 6 hours. n=4, except where indicated otherwise.

Contrary to my hypothesis, the expression of IL-6, IL-1b, iNOS, TNFα, MCP1/CCL2, and CCL4 transcripts were not significantly reduced by 1, 10, or 100 ng/ml IL-37 **(Figure 9A-F).**

In order to determine if IL-1R8 expression was affected by IL-37, BMDM were co-treated with 25ng/ml IFNγ or 20ng/ml LPS and 1, 10, and 100ng/ml recombinant IL-37 for 6 hours. The 1ng/ml IL-37 treatment alone resulted in a slight, but not significant, increase in IL-1R8. Interestingly, however, with both pro-inflammatory IFNγ and LPS treatments, IL-1R8 was consistently and significantly decreased, even with addition of 1, 10, or 100 ng/ml IL-37 (**Figure 10A).** This downregulation of IL-1R8 gene expression with IFNγ and LPS treatment was also confirmed by PCR assay **(Figure 10B).** Search of the literature revealed that others have reported similar decrease in IL-1R8 with LPS treatment in monocytes, intestinal epithelial cells, and neutrophils [34, 51, 56].

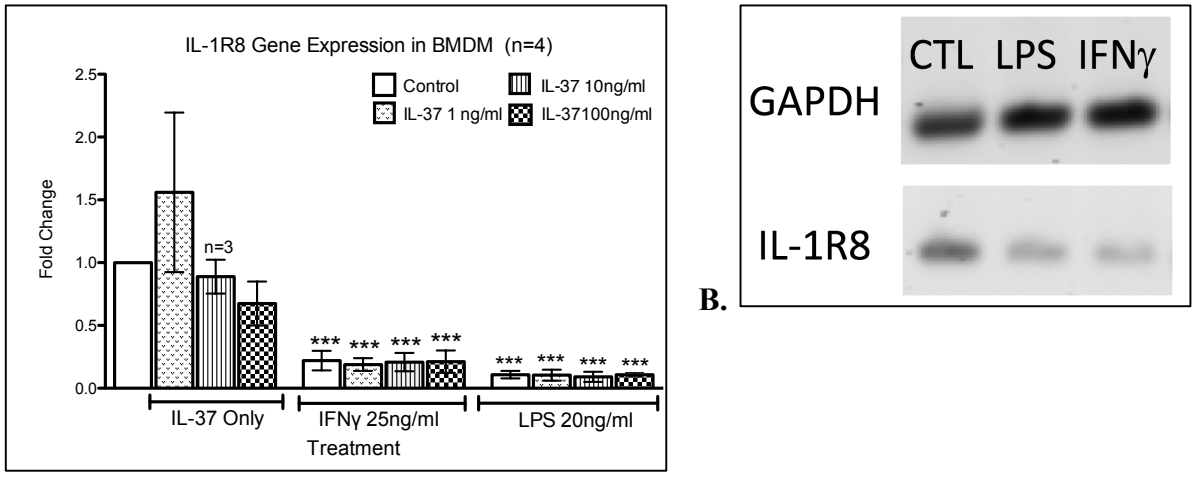

Figure 10. IL-1R8 gene expression was significantly downregulated with IFNγ and LPS treatment. (A) BMDM treated with 20ng/ml LPS and 25ng/ml IFNγ significantly downregulated IL-1R8 compared to control treatment, analyzed with RT-qPCR. ***p<0.0001, n=4, except where indicated **(B)** In BMDM, PCR shows a decrease in IL-1R8 gene expression with in BMDM with 20ng/ml LPS and 25ng/ml IFNγ treatment.

Although we were not able to show any anti-inflammatory effects of IL-37 as has been reported by many investigators, my finding that IL-1R8 is significantly reduced in macrophages in the presence of pro-inflammatory mediators led me to focus on this receptor as a means of mediating macrophage inflammation. Thus, I devised the following two specific aims to assess if macrophage inflammation can be regulated by manipulating lL-1R8.

SPECIFIC AIM I: Determine if IL-1R8 overexpression in mouse primary macrophages and mouse cell line macrophages would reduce inflammation.

a. Hypothesis

IL-1R8 in macrophages contributes to quelling inflammation under pro-inflammatory conditions.

b. Approach and Significance

The purpose of this aim was to test whether overexpressing IL-1R8 in RAW 264.7 macrophages and BMDM, *in vitro,* reduces inflammation compared to GFP DNA control. Cells were treated with pro-inflammatory (e.g., LPS, IFNγ, and TNFα) and anti-inflammatory (e.g., IL-4) mediators. Transcript levels for IL-1R8 and various inflammatory genes, (IL-6, IL-1b, iNOS, TNFα, MCP1/CCL2, CCL4), were analyzed with RT-qPCR, and IL-1R8 protein was quantified by Western blot.

1. <u>Optimized transfection of RAW 264.7 macrophages</u>

1.1 24-well plate GFP transfection optimization

In my preliminary data, IL-1R8 was consistently decreased with LPS and IFNγ pro-inflammatory stimulation. In Aim I, I shifted my attention to the role of IL-1R8 in modulating macrophage inflammation, with specific focus on whether overexpression of IL-1R8 could decrease inflammation. The first step to overexpressing IL-1R8 was to establish the optimum transfection parameters. To assess the transfection of RAW 264.7 macrophages, a CMV-driven GFP expression plasmid was used. First, $0.8X10^5$ cells were plated into a 24-well plate and the culture medium was replaced with 500µl of either antibiotic-free OptiMEM, or normal experimental medium. Different ratios of Lipofectamine 2000 (ranging from 0.4µl-4µl) and GFP plasmid DNA (0.25µg-4µg) were tested based on the manufacturer's recommendation. The

transfection efficiency was rated on a scale of the least efficient (+1) to the most efficient (+5) based on the number and brightness of GFP-positive cells. Shown in **Figure 11,** the ratio of transfection reagent to DNA with the greatest number of GFP fluorescent cells was 1.6µl of Lipofectamine 2000 to 0.8µg GFP DNA in normal experimental medium (+5). The second most highly transfected ratio was 2.4µl of Lipofectamine 2000 to 0.8µg GFP DNA in normal experimental medium (+4). The normal experimental medium allowed for higher transfection efficiency than the recommended OptiMEM medium.

Raw 264.7 Macrophage Plasmid DNA 24-well Transfection						
	1	2	3	4	5	6
A (OptiMEM)	0.4ul Lipo + 0.8 ug DNA +1	0.8ul Lipo + 0.8ug DNA +1	1.6ul Lipo + 0.8ug DNA +1	2.4ul Lipo + 0.8ug DNA +1	3.2ul Lipo + 0.8 ug DNA +1	4ul Lipo + 0.8 ugDNA +1
B (Normal Medium)	0.4ul Lipo + 0.8 ug DNA +1	0.8ul Lipo + 0.8ug DNA +1	**1.6ul Lipo + 0.8ug DNA +5**	2.4ul Lipo + 0.8ug DNA +4	3.2ul Lipo + 0.8 ug DNA +1	4ul Lipo + 0.8 ugDNA +1
C (OptiMEM)	2ul Lipo + 0.25ug DNA +1	2ul Lipo + 0.5ug DNA +1	2ul Lipo + 1ug DNA +1	2ul Lipo + 2ug DNA +1	2ul Lipo + 3ug DNA +1	2ul Lipo + 4ug DNA +1
D (Normal Medium)	2ul Lipo + 0.25ug DNA +1	2ul Lipo + 0.5ug DNA +2	2ul Lipo + 1ug DNA +3	2ul Lipo + 2ug DNA +2	2ul Lipo + 3ug DNA +1	2ul Lipo + 4ug DNA +1

Figure 11. Optimization of RAW 264.7 macrophage transfection using pcDNA3.1-GFP expression plasmid. The transfection efficiency was rated on a scale of the least transfection (+1) to the most transfection (+5). The ratio of 1.6µl of Lipofectamine 2000 to 0.8µg GFP DNA in normal experimental medium had the most effective RAW 264.7 macrophage transfection in a 24-well plate after 6 hours.

1.2 6-well plate GFP and IL-1R8 transfection optimization

Once the optimum ratio of 1.6µl of Lipofectamine 2000 to 0.8µg GFP DNA determined, the experiment was scaled up to 6-well plates. To access the transfection of GFP and IL-1R8 expression plasmids in RAW 264.7 macrophages, $4.0x10^5$ RAW 264.7 macrophages were plated into a 6-well plate in 2ml of normal experimental medium for 6 hours and the ratio of 8µl Lipofectamine 2000 to 4µg of GFP or IL-1R8 DNA per 6-well was used. These concentrations

and ratios were based on the manufacturer's protocols and the experiment described in Section 1.1. **Figure 12** shows an image of a successful GFP transfection, depicted by GFP-positive green fluorescent cells. Since IL-1R8 could not be detected by fluorescence, a PCR assay **(Figure 13)** confirmed successful IL-1R8 overexpression shown by the upregulation of IL-1R8 ~120bp.

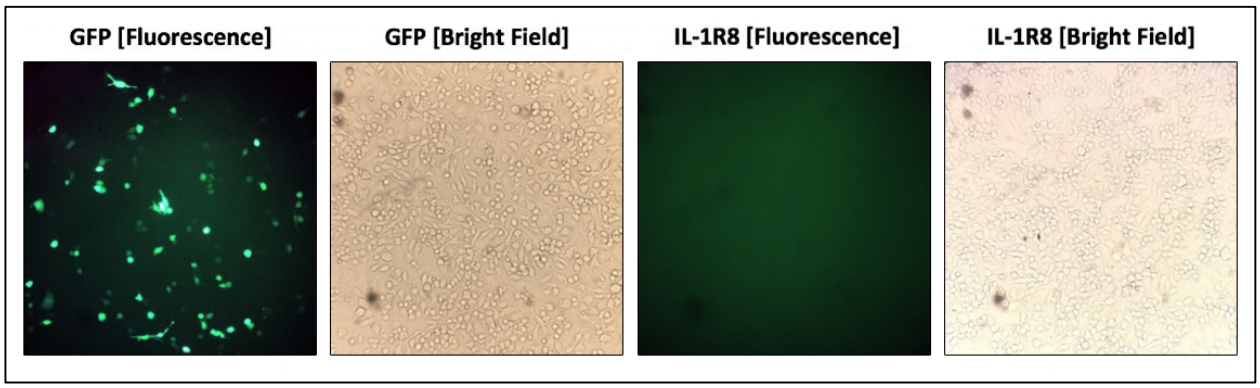

Figure 12. Images of RAW 264.7 macrophage transfection optimization using GFP and IL-1R8 expression plasmid. The optimum ratio was 8µl Lipofectamine 2000 transfecting reagent to 4µg DNA in 6-well plates with $4x10^5$ cells/well in a total of 2ml normal experimental medium for 6 hours.

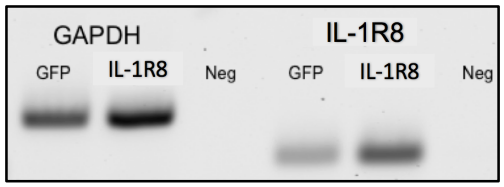

Figure 13. PCR of RAW 264.7 macrophages shows IL-1R8 overexpression. IL-1R8 transcript increased compared to GFP at ~120bp which confirms successful IL-1R8 transfection overexpression.

2. Baseline effects of IL-1R8 overexpression

2.1 RT-qPCR showed successful transfection of RAW 264.7 macrophages

After establishing the optimum GFP/IL-1R8 transfection protocol, I wanted to determine if IL-1R8 overexpression reduced inflammation. To test this, RAW 264.7 macrophages were transfected with GFP or IL-1R8 plasmid DNA in 6-well plates and the media was changed after 6 hours. The next day, the RAW 264.7 macrophages were treated with pro-inflammatory mediators, 20ng/ml LPS, 25ng/ml IFNγ, 25ng/ml TNFα or anti-inflammatory mediator, 10ng/ml

IL-4. In order to determine the baseline effects of IL-1R8 overexpression, unstimulated cells were analyzed. The RT-qPCR data for IL-1R8 transfection showed a 35-60-fold increase compared to GFP transfection **(Figure 14).**

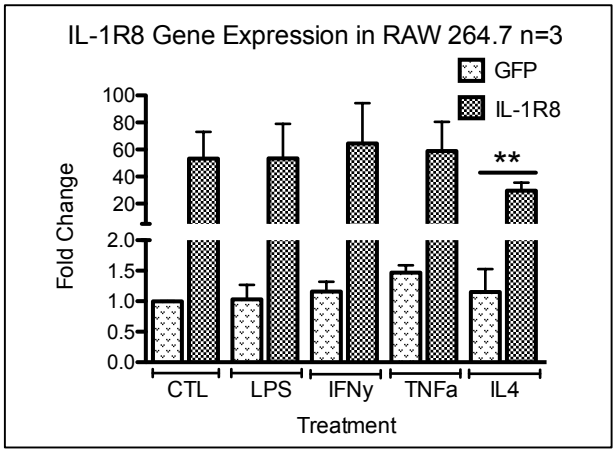

Figure 14. RT-qPCR shows successful transfection of GFP and IL-1R8 in RAW 264.7 macrophages. With 20ng/ml LPS, 25ng/ml IFNγ, 25ng/ml TNFα, or 10ng/ml IL-4 treatment, IL-1R8 gene expression showed a 35-to-60-fold change increase compared to GFP after 6 hours of transfection. There were no significant differences under LPS, IFNγ, TNFα, or IL-4 conditions. **p<0.001, n=3

2.2 Western blot showed successful transfection of IL-1R8 in RAW 264.7 macrophages

To determine if IL-1R8 protein was successfully overexpressed in RAW 264.7 macrophages, a Western blot for IL-1R8 was performed to quantify that amount of endogenous and overexpressed protein. The RAW 264.7 macrophages were transfected with GFP or IL-1R8 DNA plasmids in 6-well plates and the media was changed after 6 hours. The next day, they were treated with 20ng/ml LPS, 25ng/ml IFNγ, or 25ng/ml TNFα. In **Figure 15A,** the Western blot analysis revealed that the IL-1R8 transfection of RAW 264.7 macrophages increased IL-1R8 protein levels by 2.6-4.7 folds compared to GFP-transfected control cells. **Figure 15B** shows the total IL-1R8 protein averaged from three Western blots were not significantly affected by LPS, IFNγ and TNFα conditions compared to control.

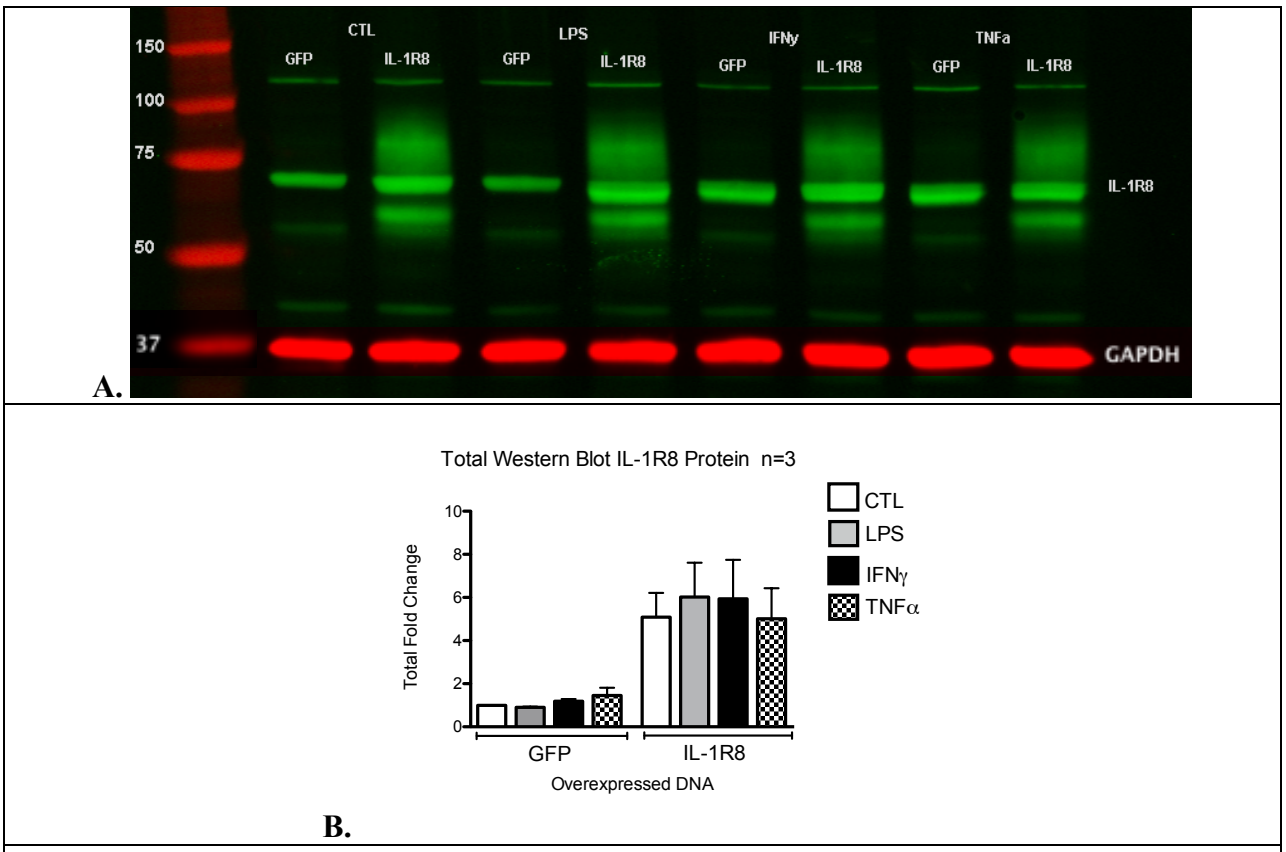

Figure 15. Western blot shows that inflammatory agents did not change IL-1R8 protein levels in IL-1R8 overexpressed RAW 264.7 macrophages. (A) Overall IL-1R8 protein levels were increased by 2.6-4.7 fold compared to GFP-transfected control cells under 20ng/ml LPS, 25ng/ml IFNγ, and 25ng/ml TNFα. n=1 **(B-C)** With GFP or IL-1R8 transfection, Control, LPS, IFNγ and TNFα conditions did not have a significant effect on IL-1R8 protein expression compared to control.

2.3 SDS PAGE In-Gel Band IL-1R8 Sequencing

To confirm that the bands seen in the Western blots are indeed that of IL-1R8, an In-gel band digestion was conducted to sequence IL-1R8 in the region corresponding to ~60kDa. I digested IL-1R8 transfected and Control treated RAW 264.7 macrophages ±PNGase F treatment (New England Lab). After reducing and alkylating the lysates, the 60kDa band that did not appear in the PNGase F treated sample was cut out and sent out to Protech Inc. to be sequenced. The company detected 35.6% or 146 out of 410 IL-1R8 amino acids which are highlighted in yellow **(Figure 16).** The six peptide sequences were analyzed in the National Center for

Biotechnology Information (NCBI) "Protein Blast" and the top results were IL-1R8/SIGIRR (single Ig IL-1-related receptor) in *mus musculus* and *homo sapiens*. The NCBI database indicated that the amino acid sequences shared similarities with the Ig superfamily and TIR2 superfamily.

MAGVCDMAPNFLSPSEDQALGLALGREVALNCTAWVFSRPQCPQPSVQWLKDGLALGNGS
HFSLHEDFWVSANFSEIVSSVLVLNLTNAEDYGTFTCSVWNVSSHSFTLWRAGPAGHVAA
VLASLLVLVVLLLVALLYVKCRLNMLLWYQDTYGEVEMNDGKLYDAYVSYSDCPEDRKFV
NFILKPQLERRRGYKLFLEDRDLLPRAEPSADLLVNLSRCRRLIVVLSDAFLSRPWCSQS
FREGLCRLLELTRRPIFITFEGQRREPIHPALRLLRQHRHLVTLVLWKPGSVTPSSDFWK
ELQLALPRKVQYRPVEGDPQTRLQDDKDPMLIVRGRAAQGRGMESELDPDPEGDLGVRGP
VFGEPPTPLQETRICIGESHGSEMDVSDLGSRNYSARTDFYCLVSEDDV

Figure 16. In-Gel band sequencing shows IL-1R8 protein. In-gel sequencing confirmed that the 60kDa band corresponded to IL-1R8. RAW 264.7 macrophages were successfully transfected with pCMV6- IL-1R8 vector at the protein level. The highlighted amino acid sequences were protein blasted and confirmed to be IL-1R8 and have similarities to the Ig and TIR2 superfamilies.

3. Effects of IL-1R8 overexpression on inflammatory gene expression with IL-37 treatment

After overexpressing IL-1R8 in RAW 264.7 macrophages and treating with 20ng/ml LPS, 25ng/ml IFNγ, 25ng/ml TNFα, or 10ng/ml IL-4, it was determined that IL-1R8 overexpression alone did not reduce inflammation **(data not shown).** Because others have shown that the IL-37/IL-18Rα/IL-1R8 tripartite complex negatively regulates inflammation, I decided to treat the IL-1R8-overexpressing macrophages with recombinant IL-37. To determine the effects of IL-1R8 overexpression with recombinant IL-37, RAW 264.7 macrophages were transfected with GFP or IL-1R8 expression plasmids and then untreated or treated with 10ng/ml recombinant IL-37. Expression levels of IL-6, iNOS, MCP1 and TNFa were analyzed via RT-qPCR, as shown below **(Figure 17).** There were no significant differences between gene expression of IL-6, iNOS, MCP1, TNFα under control conditions. However, with 10ng/ml IL-37 treatment, there was a significant (*$p<0.05$) decrease in IL-6 transcript as well as trend towards

decreasing iNOS and MCP1 supporting the hypothesis that IL-1R8 and IL-37 negatively regulate inflammation **(Figure 17B)**. The overexpression of IL-1R8 resulting in a decrease of IL-6 gene expression with IL-37 supports concept that IL-1R8 needs IL-37 to negatively regulate inflammation.

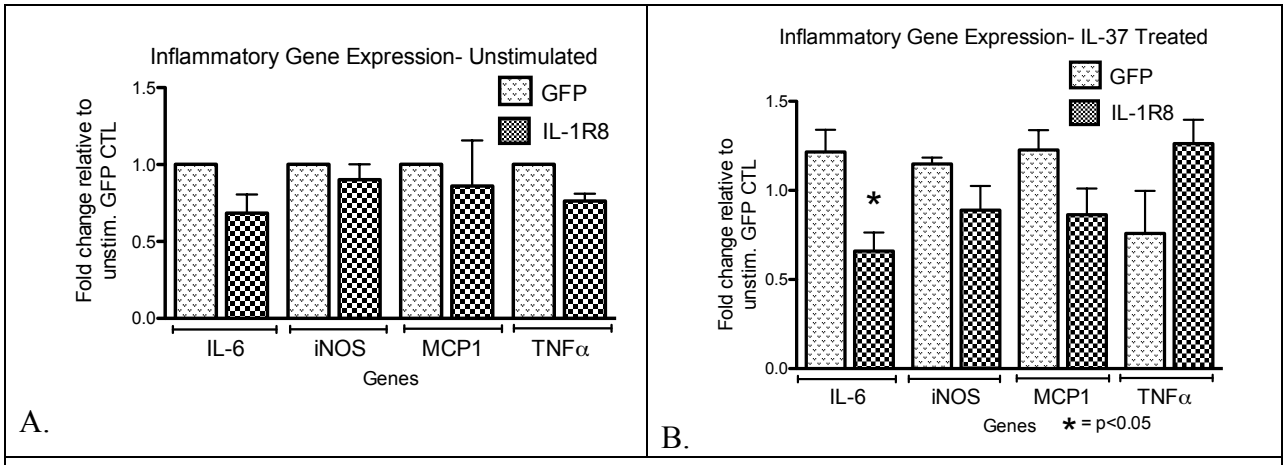

Figure 17. IL-1R8 overexpression shows signs of anti-inflammatory properties with IL-37 treatment. RAW 264.7 macrophages overexpressing IL-1R8 were treated with control or 10ng/ml IL-37**. (A)** There were no significant differences between gene expression of IL-6, iNOS, MCP1, TNFα under control conditions. **(B)** With IL-1R8 overexpression and 10ng/ml IL-37 treatment, IL-6 was significantly decreased compared to GFP control. $^{*}p<0.05$, n=3

4. Investigation of N-linked IL-1R8 Glycosylation

When analyzing the Western blots for overexpression of IL-1R8 we noticed a wide band in the region of 70-90 kDa. Because glycosylation is a common occurrence with many proteins that raises the molecular weight of the protein, I wondered whether the wide band is indeed glycosylated form of IL-1R8. In order to ascertain this I performed an enzymatic experiment as detailed below.

4.1 PNGase F Glycosidase treatment confirmed N-linked IL-1R8 Glycosylation

The RAW 264.7 macrophages were transfected with GFP or IL-1R8 in 6-well plates and the media was changed after 6 hours. The next day, they were treated with 20ng/ml LPS,

25ng/ml IFNγ, 25ng/ml TNFα or 10ng/ml IL-4. The Western blot analysis revealed a significant 70-90 kDa IL-1R8 protein band **(Figure 18)** that has rarely been described in literature.

Peptide N-glycosidase F (PNGase F) was used to determine whether IL-1R8 transfected RAW 264.7 macrophages with Control or LPS treatment were glycosylated. After treatment with PNGase F, the Western blot showed the 56-62 kDa and 70-90 kDa proteins shift to 45-49 kDa, which indicated that IL-1R8 in RAW 264.7 macrophages are glycosylated **(Figure 19)**.

A.

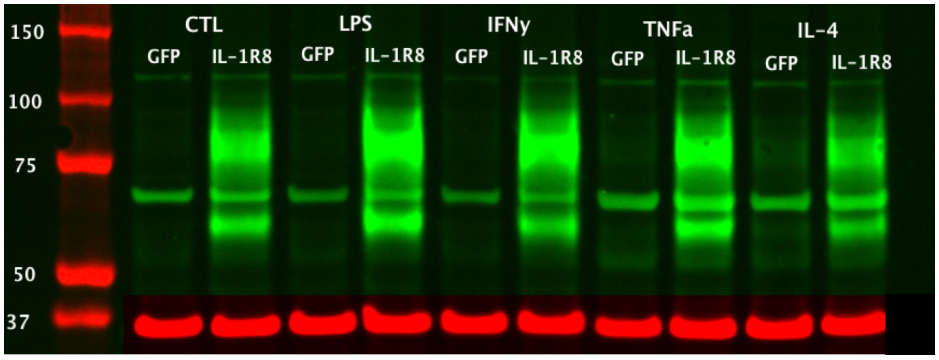

Figure 18. Western blot shows a significant IL-1R8 protein band at 70-90kDa. (A) Overall IL-1R8 protein levels are increased by 7.3-9.4 folds compared to GFP-transfected control cells.

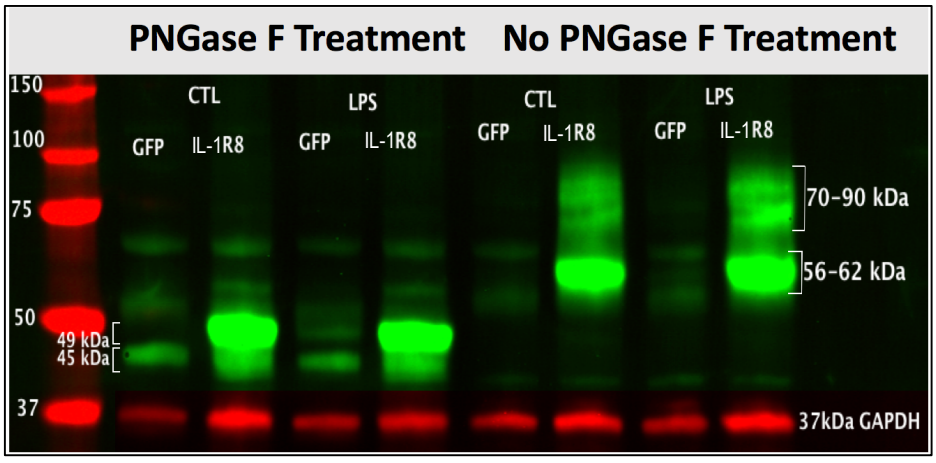

Figure 19. Treatment with Peptide N-glycosidase F (PNGase F) shows that IL-1R8 transfected RAW 264.7 macrophages are heavily N-linked glycosylated. With no PNGase F, IL-1R8 are 56-62 kDa and 70-90 kDa. With the PNGase F, the IL-1R8 protein bands shifts to 45 and 49 kDa.

5. AIM I Summary:

Using PCR, qPCR, Western blot, and In-gel sequencing, my data confirmed successful IL-1R8 overexpression in macrophages. Although IL-1R8 overexpression alone was not protective against inflammation and resulted in a significant increase in N-linked glycosylated protein, IL-1R8 overexpression with 10ng/ml IL-37 treatment was protective and significantly downregulated IL-6 gene expression, which strongly indicates that IL-37 needs to be complexed to IL-1R8 in order for its anti-inflammatory mechanism to take place.

SPECIFIC AIM II: Determine if IL-1R8 knockdown in mouse BMDM and mouse RAW 264.7 cells would enhance inflammation.

a. Hypothesis

IL-1R8 in macrophages enhances inflammation under pro-inflammatory conditions.

b. Approach and Significance

The purpose of this aim was to test whether IL-1R8 was necessary to maintain the inflammatory mechanism and cause an increase in inflammation. IL-1R8 was knocked down in macrophages with IL-1R8 siRNA. Macrophages were then treated with LPS, and the transcript levels for inflammatory genes IL-6, IL-1b, iNOS, TNFα, MCP1/CCL2, and CCL4 were analyzed via RT-qPCR and IL-1R8 protein was quantified with Western blot.

1. <u>Optimized siRNA knockdown of IL-1R8 in BMDM</u>

1.1 Time point and concentration

To determine whether knocking down IL-1R8 would cause an increase in inflammation, the optimum siRNA treatment time point and concentration needed to be determined. In **Figure 20,** BMDM were plated at $3.5X10^6$ for 24 with 50nM and100nM of siRNA. At 24 hours with 100nM of siRNA, the PCR showed an effective inhibition of IL-1R8 expression compared to 50nM siRNA and Scrambled treatment at 24 hours.

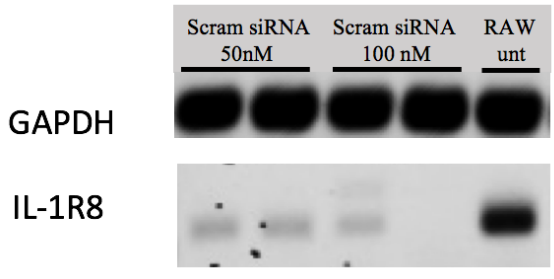

Figure 20. PCR of optimized IL-1R8 knocked down with siRNA in BMDM. At 24 hours with 100nM of siRNA effectively knocked down IL-1R8 compared to 50nM siRNA and Scrambled treatment at 24 hours. GAPDH gene expression is consistent throughout the samples.

2. Effects of IL-1R8 siRNA on BMDM treated with LPS and/or IL-37

2.1 RT-qPCR of siRNA knockdown-LPS stimulated with IL-37 in BMDM

To determine the effect of IL-1R8 siRNA knockdown with recombinant IL-37, BMDM were transfected with 50nM Scrambled or IL-1R8 siRNA in 6-well plate for 24hours. Then, the BMDM were treated with 50ng/ml LPS ±10ng/ml IL-37 for an additional 24hrs. **In Figure 21A**, the RT-qPCR data are shown for siRNA downregulated IL-1R8 in the Control and IL-37 treated BMDM. In **Figure 21B-C**, with the downregulation of IL-1R8, IL-6 and IL-1b increased with LPS and IL-37/LPS treatment. This adds to the mounting support that IL-1R8 is necessary for negative regulation of inflammation.

A.

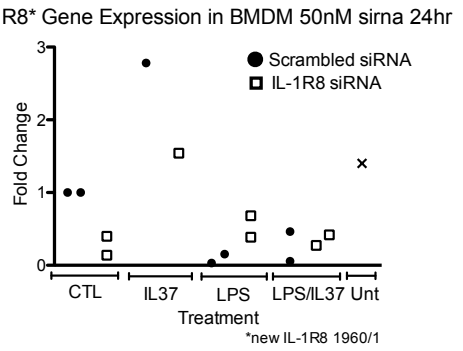

B.

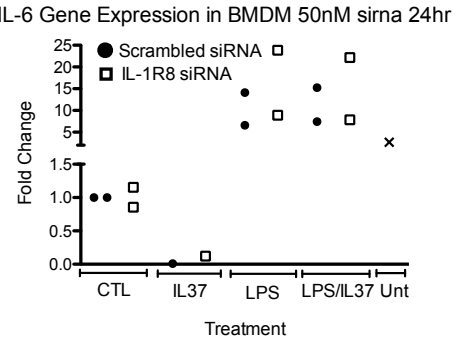

C.

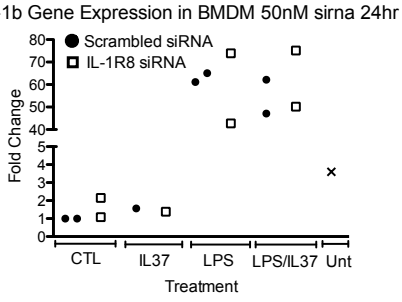

Figure 21. IL-1R8 knockdown in BMDM led to an increase in inflammatory gene expression. (A) In a 6-well plate, 50nM of IL-1R8 siRNA transfected for 24 hours downregulated IL-1R8 in the Control and IL-37 treated BMDM.
(B-C) siRNA downregulation of IL-1R8 showed signs of increased IL-6 and IL-1b gene expression with 50ng/ml LPS ± 10ng/ml IL-37 treatment. n=2 biological replicates, #: n=1

3. Optimized siRNA knockdown of in RAW 264.7 Macrophages

To determine if protein levels of IL-1R8 were successfully knocked down in RAW 264.7 macrophages, Western blots were performed to assess IL-1R8 protein levels. RAW 264.7 macrophages were transfected with 50nM Scrambled or IL-1R8 siRNA in 6-well plate for 48hours. Then, the RAW 264.7 macrophages were treated with 1μg/ml LPS or 10ng/ml IL-37 for an additional 24hrs. In **Figure 22A**, the Western blots with IL-1R8 siRNA transfection showed successful IL-1R8 knockdown with control treatment, LPS, and IL-37 treatments. Glycosylated IL-1R8 was shown at 77-85 kDa and unglycosylated IL-1R8 at 50-55kDa. The overall IL-1R8 protein (**Figure 22B)** was decreased with IL-1R8 siRNA consistently under control, LPS and IL-37 treatment conditions.

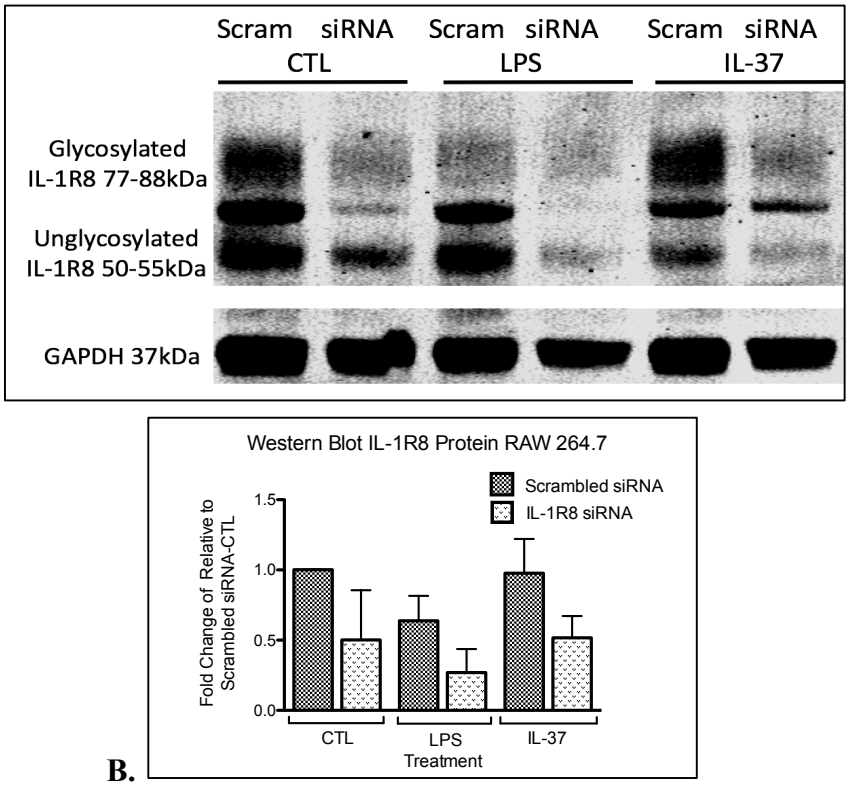

Figure 22. Western blot of RAW 264.7 cells shows successful knockdown of IL-1R8 with siRNA. (A-B) IL-1R8 in RAW 264.7 cells were knocked down with 50nM siRNA in 6-well plate for 48hours. Then, treated with 1μg/ml LPS or 10ng/ml IL-37 for 24hrs. Glycosylated and unglycosylated IL-1R8 protein is shown at 77-85 kDa and 50-55kDa, respectively. With LPS treatment, IL-1R8 was slightly downregulated. The housekeeping gene is GAPDH at 37kDa. n=2

4. <u>Effects of IL-1R8 siRNA on RAW 264.7 inflammation</u>

Next, I sought to determine the effect of IL-1R8 siRNA knockdown at transcript level in RAW 264.7 macrophages, which were transfected with 50nM Scrambled or IL-1R8 siRNA in 6-well plate for 48hours. Then, the RAW 264.7 macrophages were treated with 1μg/ml LPS ±10ng/ml IL-37 for an additional 24hrs. As shown in the figure below **(Figure 23),** gene expression for IL-6, IL-1b, TNFα, and MCP1/CCL2 were all consistently upregulated with IL-1R8 knockdown under control, LPS, and LPS/IL-37 treatment conditions. These data suggest that IL-1R8 can resolve inflammation, particularly under pro-inflammatory conditions as seen with LPS treatment.

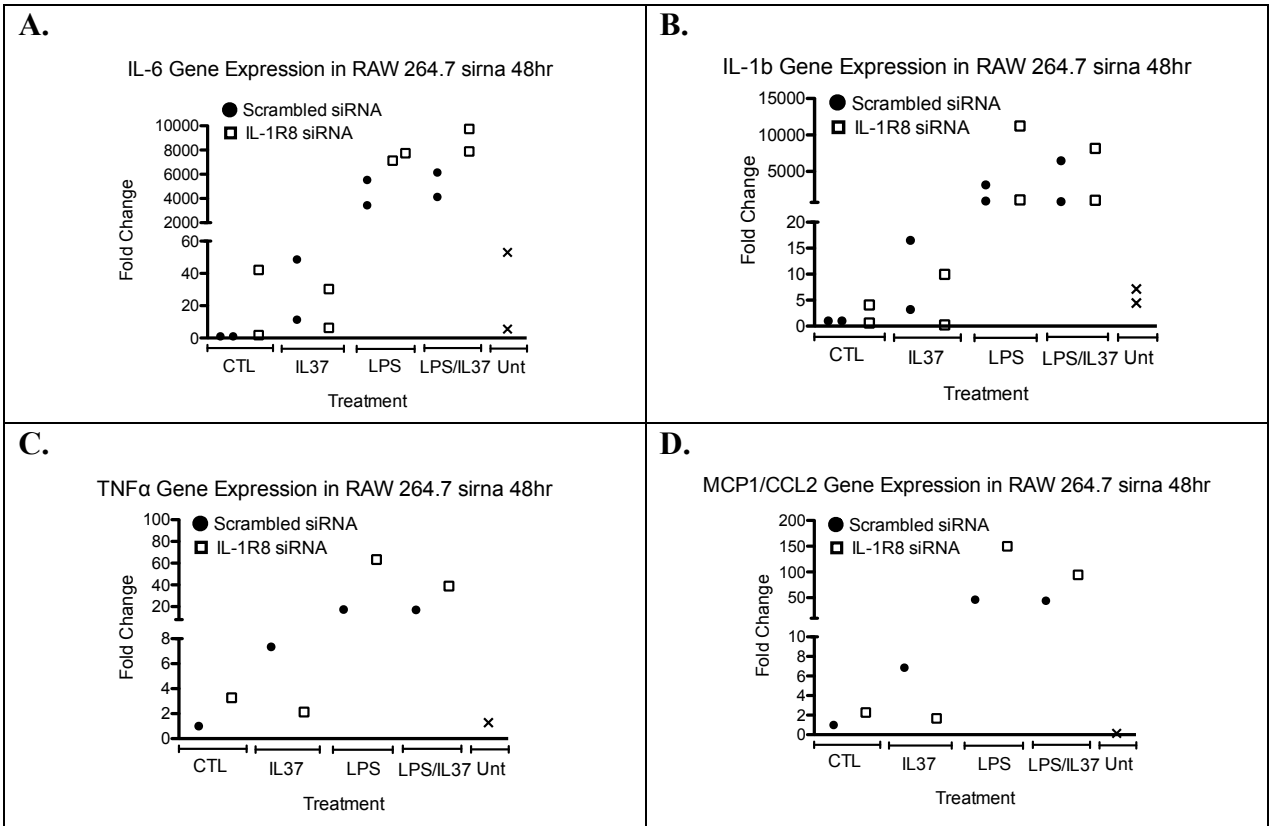

Figure 23. RT-qPCR shows that IL-1R8 siRNA knockdown with LPS ± IL-37 suggests an increase in inflammation. (A-D) RAW 264.7 Macrophages in a 6-well plate transfected with 50nM IL-1R8 siRNA for 48hours with 1μg/ml LPS or LPS+10ng/ml treatment suggests an increase in IL-6, IL-1b, TNFα, and MCP1/CCL2 gene expression. A-B. n=2; C-D. n=1

5. AIM II Summary:

Using PCR, qPCR, and Western blot, my data confirmed IL-1R8 transcript and protein knockdown in macrophages treated with IL-1R8 siRNA. IL-1R8 knockdown with LPS ± IL-37 treatment showed signs of enhanced IL-6, IL-1b, and TNFα gene expression. This supports my hypothesis that IL-1R8 participates in attenuating inflammation in macrophages.

CHAPTER 4: DISCUSSION & FUTURE DIRECTIONS

1. Summary and interpretation of results

1.1. Preliminary Data: Determine the effect of recombinant IL-37 in macrophages

The experiments in this thesis investigated the role of IL-1R8 and IL-37 in modulating macrophage inflammation. My preliminary data determined the optimum conditions for pre- versus co-treatment of LPS and IL-37, time point, and concentration of pro-inflammatory markers and IL-37. Using recombinant IL-37 BMDM did not prove to be protective against LPS- and IFNγ-stimulated inflammation, although other studies have shown that picomolar concentrations of IL-37 ranging from 10-0.1 ng/ml prove to be protective against inflammation [43]. Interestingly, however, under pro-inflammatory conditions, induced by IFNγ and LPS treatments, IL-1R8 was significantly decreased with 1, 10, 100 ng/ml recombinant IL-37.

1.2 AIM I: Determine if IL-1R8 overexpression in mouse primary macrophages and mouse cell line macrophages would reduce inflammation.

The decrease in IL-1R8 under pro-inflammatory conditions led me to investigate IL-1R8's anti-inflammatory properties. In AIM I, experiments were conducted to optimize IL-1R8 overexpression transfection in both primary bone marrow derived macrophages and RAW 264.7 macrophages. The optimum concentration was determined to be 8μl of Lipofectamine 2000 to 4μg of GFP or IL-1R8 DNA. Initially, with IL-1R8 overexpression and pro-inflammatory conditions induced by LPS, IFNγ, and TNFα in RAW 264.7 macrophages, the RT-qPCR analysis showed no significant protection against inflammation, as noted by upregulation of IL-6, IL-1b, and iNOS gene expression in IL-1R8-overexpressing cells. The Western blot analysis of RAW 264.7 macrophages showed successful IL-1R8 overexpression. Interestingly, all three trials presented with smeared protein from 65kDa-90kDa. As others have shown that IL-1R8 can

be heavily glycosylated, [45, 48, 51], I took the steps to confirm this by excising the 60kDa band from the SDS-PAGE gel and having it sequenced by Protech, Inc **(Figure 16).** They were able to verify that 6 peptide sequences were that of IL-1R8, which confirm the IL-1R8 overexpression.

The experiments in which only IL-1R8 overexpression was achieved without additional treatments did not show protection against inflammation. This prompted me to incorporate recombinant IL-37 as it might be that IL-37 binding to IL-1R8 is necessary for the anti-inflammatory activity to take place. In support of this, other investigators have found that, IL-37 binds to IL-18Rα, which associates with IL-1R8 to downregulate inflammation [43, 49]. With IL-1R8 overexpression and 10ng/ml IL-37 treatment in RAW 264.7 macrophages, there was a significant downregulation of IL-6 gene expression **(Figure 17B).** As hypothesized, these results suggested that IL-37 binding to IL-1R8 is needed for this complex to exert its anti-inflammatory properties in macrophages.

The Western blot with IL-37 treatment showed a significant increase in IL-1R8 to confirm overexpression and revealed that IL-1R8 is expressed in glycosylated form with various degrees of glycosylation weighing around 70-90kDa. The protein bands visible at 56-62kDa and 70-90kDa were confirmed to be N-linked glycosylated with PNGase F treatment **(Figure 19).** I also confirmed the Western blot bands to be IL-1R8 by detecting the MYC-tagged pCMV6 IL-1R8 vector (data not shown).

1.3 AIM II: Determine if IL-1R8 knockdown in mouse BMDM and mouse RAW 264.7 cells would enhance inflammation.

Once the overexpression of IL-1R8 in RAW 264.7 macrophages was confirmed to downregulate inflammation with IL-37, the AIM II experiments were conducted to determine whether IL-1R8 was necessary to protect against inflammation by knocking down IL-1R8 in

macrophages using siRNA. The optimum condition for the siRNA-mediated knockdown was determined to be 24hours with 100nM siRNA transfection in both primary bone marrow derived macrophages **(Figure 20)** and 48hours with 50nM siRNA in RAW 264.7 macrophages **(Figure 22).** Initially, IL-1R8 siRNA knockdown was tested in BMDM with pro-inflammatory LPS. The data confirmed that LPS downregulates IL-1R8 expression (seen with scrambled siRNA results, Figure 21A). The RT-qPCR analysis showed an increasing trend of IL-6, but not IL-1b with LPS and LPS/IL-37 treatment, suggesting IL-1R8's role in negatively regulating inflammation. The same experiment was conducted with RAW 264.7 macrophages also showed an upregulation of IL-6 gene expression with LPS or LPS/IL-37 treatment (**Figure 23** p=0.11). Similar trends were seen in gene expression of IL-1b, MCP1, and TNFα, all indicating heightened inflammation with IL-1R8 siRNA knockdown **(Figure 23).** Interestingly, the Western blot confirmed downregulation of IL-1R8, but mainly in the glycosylated 77-88 kDa region (**Figure 22A).** This further supports my hypothesis that IL-1R8 is necessary to resolve inflammation in macrophages.

2. Importance of IL-1R8 in preventing inflammation

2.1. Role in Disease

IL-1R8, a member of the IL-1 and TLR family, played a vital role in maintaining homeostasis, protecting against infection, and modulating inflammation [47, 57]. There was evidence that IL-1R8 negatively regulated inflammation in various inflammatory, autoimmune, cardiovascular and neuronal disease, as well as during infections [58-61]. In rheumatoid arthritis, for example, IL-1R8 suppresses the release of cytokines in human synovial cells [35]. When mice were infected with *Mycobacterium tuberculosis,* IL-1R8$^{-/-}$ mice displayed a higher mortality than the control group [62]. In post-ischemic renal failure, IL-1R8 deficiency was associated

with an increase in renal injury due to increased cytokine release and inflammation [63]. In brain cells, such as, neurons, astrocytes, and microglia, IL-1R8 has been shown to regulate LPS-activated inflammation. When mice are made to be deficient in IL-1R8, there is an increase in cytokine release and excessive inflammatory response to LPS [64]. Also, in Alzheimer's disease, IL-1R8 negatively regulates β-amyloid peptide-induced TLR2 signaling in the brain which is the main contributor to neuronal plaque accumulations [65]. In addition, IL-1R8 plays a crucial role in maintaining intestinal homeostasis. In the intestinal colitis model, IL-1R8$^{-/-}$ mice were shown to have dramatically increased intestinal inflammation and bleeding, as well as, compromised survival [66, 67]. Inflammation is necessary to fight off infection and disease, but when unregulated, cancer and tumors can develop. IL-1R8 has been shown to protect against colon cancer related inflammation [68]. Lastly, in combination with IL-37, IL-1R8 has protective properties in cardiovascular diseases, such as atherosclerosis and myocardial infarction [69, 70].

3. Regulation of IL-1R8 under inflammatory conditions

3.1 IL-1R8 downregulation by LPS

Treatment with pro-inflammatory mediators, such as, LPS, has been shown to downregulate IL-1R8 in monocytes, intestinal epithelial cells, and neutrophils [34, 56]. In intestinal epithelial cells from ulcerative colitis patients, IL-1R8 (SIGIRR) negatively regulated Toll-like receptor (TLR)-4-signaling. LPS treatment induced the downregulation of IL-1R8 which decreased SP1 binding at the IL-1R8 promoter [34]. LPS was shown to downregulate IL-1R8 in both monocytes and neutrophils, which led to increased inflammation. Furthermore, it was shown that TLR4-dependent p38 MAPK pathway contributes to the LPS-mediated reduction of IL-1R8. In support of the above-mentioned studies, my work showed a significant downregulation of IL-1R8 with LPS (**Figure 10A**). By suppressing the LPS activated TLR4-

dependent p38 MAPK pathway, this may help decrease downregulation of IL-1R8 to help prevent inflammation in various disease.

3.2 IL-1R8 Glycosylation

Glycosylation is a post-translational modification that regulates protein folding and trafficking. There are 5 potential N-glycosylation sites on human IL-1R8 and 4 on mouse IL-1R8 [47, 48, 51, 54]. The size of IL-1R8 protein ranges from unglycosylated 44kDa to glycosylated 90kDa. The range is likely due to the addition of glycans in various amounts at IL-1R8 $^{N31/73/86/102S}$[51].

N-linked glycosylation begins in the ER where high mannose modification is added to the nascent protein and then transported to the Golgi apparatus for additional modification. Hypothetically, dysregulation of glycosylation can lead to spontaneous intestinal inflammation, irregular intracellular trafficking and protein folding, and the promotion of cancer. [48, 51, 53]. Investigating the role and function of glycosylation in BMDM and RAW 264.7 macrophages may provide insight into IL-1R8's role in inflammation in the context of atherosclerosis.

4. Therapeutic Potential for IL-37 and IL-1R8 in inflammatory diseases

4.1. IL-37 Homodimerization effect on Anti-Inflammatory Properties

IL-37 is a potential therapeutic target for suppressing inflammation in diseases, such as, atherosclerosis and other immune diseases. Under experimental *in vitro* and *in vivo* conditions, the isoform IL-37b was reported to form homodimers which suggested the biological importance of IL-37 processing. When overexpressing IL-37b in HEK 293 cells, pro and mature isomers formed, which had different estimated dimerization association constants of mature 5nM for mature and 4uM for pro IL-37b [16, 71]. My data show that in RAW 264.7 cells, the molecular weight of IL-37b protein is 25kDa, but in PBMCs, the molecular weight increases to 45kDa. The

immunoblots were conducted under non-reducing conditions to suggest possiblevIL-37 homodimerization [18].

In 2017, IL-37b was crystallized, which demonstrated that IL-37 forms a head to head homodimer. This head to head orientation was unique in the IL-1 superfamily of cytokines. Treating THP-1 cell lines with pro-inflammatory mediator, LPS, monomeric IL-37 variants resulted in a 2.3 IL-1β fold change improvement of anti-inflammatory activity compared to natural IL-37b. In an *in vivo* endotoxic shock mouse model, injection of recombinant IL-37 monomeric variants resulted in a 13-fold change greater improvement of endotoxic shock and decrease of IL-1β in plasma [72].

Homodimerization regulation of IL-37 plays an important role in dampening inflammation. In **Figure 9A-F,** treatment with recombinant IL-37 did not effectively protect against inflammation as indicated in previous work [18, 38]. This could be due to the formation of head to head dimerization which may have inhibited the protective effect of recombinant IL-37. Regulating the ratio between IL-37 monomers versus homodimers, especially in atherosclerotic macrophages may be a potential therapeutic target to suppress excessive inflammation in the arterial necrotic core. This would ultimately decrease atherosclerosis and the incidence of heart attacks and stroke.

5. Limitations and future directions

After successfully overexpressing and knocking down IL-1R8 in primary and RAW 264.7 macrophages, one of the limitations is that only male mice were used. Future experiments designed to investigate both male and female mice *in vitro* and *in vivo* will allow us to see if there are any differences between sex. Also, in IL-1R8 overexpressed or knocked down mice, the glycosylation sites on IL-1R8 *in-vitro* and *in vivo* with IL-37 treatment may reveal the

importance of glycosylation in negatively regulating inflammation. Additional SDS PAGE In-gel band sequencing of IL-1R8 needs to be conducted to confirm IL-1R8 from 46kDa- 90kDa. Treating IL-1R8 overexpressed and knocked down macrophages with monomeric IL-37 mutant variants [72] would further determine the function of homodimerized IL-37 and may reveal why we did observe the purported anti-inflammatory effects of IL-37. Lastly, exploring IL-1R8 localization with flow cytometry would allow us to learn more about the receptor membrane presentation.

LITERATURE CITED:

1. *World Heath Organization Cardiovascular diseases (CVDs) Fact Sheet*. 2017 [cited 2017 May 20]; May 2017:[Available from: http://www.who.int/mediacentre/factsheets/fs317/en/.
2. Roth, G.A., et al., *Global and regional patterns in cardiovascular mortality from 1990 to 2013.* Circulation, 2015. **132**(17): p. 1667-78.
3. Hansson, G.K., *Inflammation, atherosclerosis, and coronary artery disease.* N Engl J Med, 2005. **352**(16): p. 1685-95.
4. Bloom, D., *The Global Economic Burden of Noncummunicable Diseases.* World Economic Forum, 2011.
5. CDC. *Heart Disease Facts*. 2017 [cited 2017 May 1]; Available from: https://www.cdc.gov/heartdisease/facts.htm.
6. Benjamin, E.J., et al., *Heart Disease and Stroke Statistics-2017 Update: A Report From the American Heart Association.* Circulation, 2017. **135**(10): p. e146-e603.
7. CDC. *Interactive Atlas of Heart Disease and Stroke*. 2015 [cited 2017 June 24]; Available from: https://nccd.cdc.gov/DHDSPAtlas/?state=State&ol=[10].
8. Association, A.H., *Cardiovascular Disease: A costly burden for america projections through 2035*, T.A.H.A.O.o.F. Advocacy, Editor. 2017.
9. Goldstein, J.L. and M.S. Brown, *Regulation of low-density lipoprotein receptors: implications for pathogenesis and therapy of hypercholesterolemia and atherosclerosis.* Circulation, 1987. **76**(3): p. 504-7.
10. Fryar, C., T. Chen, and X. Li, *Prevalence of Uncontrolled Risk Factors for Cardiovascular Disease: United States, 1999–2010*, in *NCHS data brief, no 103*. 2012, National Center for Health Statistics: Hyattsville, MD.
11. Claria, J., et al., *New insights into the role of macrophages in adipose tissue inflammation and Fatty liver disease: modulation by endogenous omega-3 Fatty Acid-derived lipid mediators.* Front Immunol, 2011. **2**: p. 49.
12. Ellulu, M.S., et al., *Atherosclerotic cardiovascular disease: a review of initiators and protective factors.* Inflammopharmacology, 2016. **24**(1): p. 1-10.
13. Wagsater, D., et al., *MMP-2 and MMP-9 are prominent matrix metalloproteinases during atherosclerosis development in the Ldlr(-/-)Apob(100/100) mouse.* Int J Mol Med, 2011. **28**(2): p. 247-53.
14. Moore, K.J. and I. Tabas, *Macrophages in the pathogenesis of atherosclerosis.* Cell, 2011. **145**(3): p. 341-55.
15. Kumar, S., et al., *Identification and initial characterization of four novel members of the interleukin-1 family.* J Biol Chem, 2000. **275**(14): p. 10308-14.
16. Boraschi, D., et al., *IL-37: a new anti-inflammatory cytokine of the IL-1 family.* Eur Cytokine Netw, 2011. **22**(3): p. 127-47.
17. Dinarello, C.A., et al., *Suppression of innate inflammation and immunity by interleukin-37.* Eur J Immunol, 2016. **46**(5): p. 1067-81.
18. Nold, M.F., et al., *IL-37 is a fundamental inhibitor of innate immunity.* Nat Immunol, 2010. **11**(11): p. 1014-22.
19. Weidlich, S., et al., *Intestinal Expression of the Anti-inflammatory Interleukin-1 Homologue IL-37 in Pediatric Inflammatory Bowel Disease.* J Pediatr Gastroenterol Nutr, 2014.

20. Teng, X., et al., *IL-37 ameliorates the inflammatory process in psoriasis by suppressing proinflammatory cytokine production.* J Immunol. **192**(4): p. 1815-23.
21. Zhao, P.W., et al., *Plasma levels of IL-37 and correlation with TNF-alpha, IL-17A, and disease activity during DMARD treatment of rheumatoid arthritis.* PLoS One, 2014. **9**(5): p. e95346.
22. Ye, L., et al., *IL-37 inhibits the production of inflammatory cytokines in peripheral blood mononuclear cells of patients with systemic lupus erythematosus: its correlation with disease activity.* J Transl Med, 2014. **12**: p. 69.
23. Imaeda, H., et al., *Epithelial expression of interleukin-37b in inflammatory bowel disease.* Clin Exp Immunol. **172**(3): p. 410-6.
24. Hojen, J.F., et al., *Interleukin-37 Expression Is Increased in Chronic HIV-1-Infected Individuals and Is Associated with Inflammation and the Size of the Total Viral Reservoir.* Mol Med, 2015. **21**: p. 337-45.
25. Huang, Z., et al., *IL-37 Expression is Upregulated in Patients with Tuberculosis and Induces Macrophages Towards an M2-like Phenotype.* Scand J Immunol, 2015. **82**(4): p. 370-9.
26. Ji, Q., et al., *Elevated plasma IL-37, IL-18, and IL-18BP concentrations in patients with acute coronary syndrome.* Mediators Inflamm, 2014. **2014**: p. 165742.
27. Li, W., et al., *Interleukin-37 elevation in patients with atrial fibrillation.* Clin Cardiol, 2017. **40**(2): p. 66-72.
28. Wu, B., et al., *Interleukin-37 ameliorates myocardial ischaemia/reperfusion injury in mice.* Clin Exp Immunol, 2014. **176**(3): p. 438-51.
29. Yang, Y., et al., *IL-37 inhibits IL-18-induced tubular epithelial cell expression of pro-inflammatory cytokines and renal ischemia-reperfusion injury.* Kidney Int, 2015. **87**(2): p. 396-408.
30. Zhu, R., et al., *Interleukin-37 and Dendritic Cells Treated With Interleukin-37 Plus Troponin I Ameliorate Cardiac Remodeling After Myocardial Infarction.* J Am Heart Assoc, 2016. **5**(12).
31. Xu, D., et al., *Effects of interleukin-37 on cardiac function after myocardial infarction in mice.* Int J Clin Exp Pathol, 2015. **8**(5): p. 5247-51.
32. Zeng, Q., et al., *Interleukin-37 suppresses the osteogenic responses of human aortic valve interstitial cells in vitro and alleviates valve lesions in mice.* Proceedings of the National Academy of Sciences of the United States of America, 2017. **114**(7): p. 1631-1636.
33. Chai, M., et al., *The Protective Effect of Interleukin-37 on Vascular Calcification and Atherosclerosis in Apolipoprotein E-Deficient Mice with Diabetes.* J Interferon Cytokine Res, 2015. **35**(7): p. 530-9.
34. Kadota, C., et al., *Down-regulation of single immunoglobulin interleukin-1R-related molecule (SIGIRR)/TIR8 expression in intestinal epithelial cells during inflammation.* Clin Exp Immunol, 2010. **162**(2): p. 348-61.
35. Drexler, S.K. and B.M. Foxwell, *The role of toll-like receptors in chronic inflammation.* Int J Biochem Cell Biol, 2010. **42**(4): p. 506-18.
36. Bulau, A.M., et al., *In vivo expression of interleukin-37 reduces local and systemic inflammation in concanavalin A-induced hepatitis.* ScientificWorldJournal, 2011. **11**: p. 2480-90.

37. Liu, K., et al., *IL-37 increased in patients with acute coronary syndrome and associated with a worse clinical outcome after ST-segment elevation acute myocardial infarction.* Clin Chim Acta, 2017. **468**: p. 140-144.
38. Nold-Petry, C.A., et al., *IL-37 requires the receptors IL-18Ralpha and IL-1R8 (SIGIRR) to carry out its multifaceted anti-inflammatory program upon innate signal transduction.* Nat Immunol, 2015. **16**(4): p. 354-65.
39. Bufler, P., et al., *A complex of the IL-1 homologue IL-1F7b and IL-18-binding protein reduces IL-18 activity.* Proc Natl Acad Sci U S A, 2002. **99**(21): p. 13723-8.
40. Bufler, P., et al., *Interleukin-1 homologues IL-1F7b and IL-18 contain functional mRNA instability elements within the coding region responsive to lipopolysaccharide.* Biochem J, 2004. **381**(Pt 2): p. 503-10.
41. Dinarello, C.A., *Biologic basis for interleukin-1 in disease.* Blood, 1996. **87**(6): p. 2095-147.
42. Bulau, A.M., et al., *Role of caspase-1 in nuclear translocation of IL-37, release of the cytokine, and IL-37 inhibition of innate immune responses.* Proceedings of the National Academy of Sciences of the United States of America, 2014. **111**(7): p. 2650-5.
43. Li, S., et al., *Extracellular forms of IL-37 inhibit innate inflammation in vitro and in vivo but require the IL-1 family decoy receptor IL-1R8.* Proc Natl Acad Sci U S A, 2015. **112**(8): p. 2497-502.
44. Nold-Petry, C.A., et al., *IL-37 requires the receptors IL-18R[alpha] and IL-1R8 (SIGIRR) to carry out its multifaceted anti-inflammatory program upon innate signal transduction.* Nat Immunol, 2015. **16**(4): p. 354-365.
45. Thomassen, E., B.R. Renshaw, and J.E. Sims, *Identification and characterization of SIGIRR, a molecule representing a novel subtype of the IL-1R superfamily.* Cytokine, 1999. **11**(6): p. 389-99.
46. Garlanda, C., et al., *Increased susceptibility to colitis-associated cancer of mice lacking TIR8, an inhibitory member of the interleukin-1 receptor family.* Cancer Res, 2007. **67**(13): p. 6017-21.
47. Garlanda, C., H.J. Anders, and A. Mantovani, *TIR8/SIGIRR: an IL-1R/TLR family member with regulatory functions in inflammation and T cell polarization.* Trends Immunol, 2009. **30**(9): p. 439-46.
48. Lech, M., et al., *Different roles of TiR8/Sigirr on toll-like receptor signaling in intrarenal antigen-presenting cells and tubular epithelial cells.* Kidney Int, 2007. **72**(2): p. 182-92.
49. Molgora, M., et al., *Regulatory Role of IL-1R8 in Immunity and Disease.* Front Immunol, 2016. **7**: p. 149.
50. Wald, D., et al., *SIGIRR, a negative regulator of Toll-like receptor-interleukin 1 receptor signaling.* Nat Immunol, 2003. **4**(9): p. 920-7.
51. Zhao, J., et al., *Human Colon Tumors Express a Dominant-Negative Form of SIGIRR That Promotes Inflammation and Colitis-Associated Colon Cancer in Mice.* Gastroenterology, 2015. **149**(7): p. 1860-1871 e8.
52. Weber, A.N., M.A. Morse, and N.J. Gay, *Four N-linked glycosylation sites in human toll-like receptor 2 cooperate to direct efficient biosynthesis and secretion.* J Biol Chem, 2004. **279**(33): p. 34589-94.
53. Scheiffele, P., J. Peranen, and K. Simons, *N-glycans as apical sorting signals in epithelial cells.* Nature, 1995. **378**(6552): p. 96-8.

54. Magnelli, P., A. Bielik, and E. Guthrie, *Identification and characterization of protein glycosylation using specific endo- and exoglycosidases.* Methods Mol Biol, 2012. **801**: p. 189-211.
55. McNamee, E.N., et al., *Interleukin 37 expression protects mice from colitis.* Proc Natl Acad Sci U S A, 2011. **108**(40): p. 16711-6.
56. Ueno-Shuto, K., et al., *Lipopolysaccharide decreases single immunoglobulin interleukin-1 receptor-related molecule (SIGIRR) expression by suppressing specificity protein 1 (Sp1) via the Toll-like receptor 4 (TLR4)-p38 pathway in monocytes and neutrophils.* J Biol Chem, 2014. **289**(26): p. 18097-109.
57. Li, X. and J. Qin, *Modulation of Toll-interleukin 1 receptor mediated signaling.* J Mol Med (Berl), 2005. **83**(4): p. 258-66.
58. Liew, F.Y., N.I. Pitman, and I.B. McInnes, *Disease-associated functions of IL-33: the new kid in the IL-1 family.* Nat Rev Immunol, 2010. **10**(2): p. 103-10.
59. Dinarello, C.A., *Interleukin-1 in the pathogenesis and treatment of inflammatory diseases.* Blood, 2011. **117**(14): p. 3720-32.
60. Krelin, Y., et al., *Interleukin-1beta-driven inflammation promotes the development and invasiveness of chemical carcinogen-induced tumors.* Cancer Res, 2007. **67**(3): p. 1062-71.
61. Towne, J.E. and J.E. Sims, *IL-36 in psoriasis.* Curr Opin Pharmacol, 2012. **12**(4): p. 486-90.
62. Garlanda, C., et al., *Damping excessive inflammation and tissue damage in Mycobacterium tuberculosis infection by Toll IL-1 receptor 8/single Ig IL-1-related receptor, a negative regulator of IL-1/TLR signaling.* J Immunol, 2007. **179**(5): p. 3119-25.
63. Lech, M., et al., *Resident dendritic cells prevent postischemic acute renal failure by help of single Ig IL-1 receptor-related protein.* J Immunol, 2009. **183**(6): p. 4109-18.
64. MB, W., et al., *SIGIRR modulates the inflammatory response in the brain.* Brain Behav Immun
, 2010. **24**: p. 985–95.
65. Costello, D.A., D.G. Carney, and M.A. Lynch, *alpha-TLR2 antibody attenuates the Abeta-mediated inflammatory response in microglia through enhanced expression of SIGIRR.* Brain Behav Immun, 2015. **46**: p. 70-9.
66. Garlanda, C., et al., *Intestinal inflammation in mice deficient in Tir8, an inhibitory member of the IL-1 receptor family.* Proc Natl Acad Sci U S A, 2004. **101**(10): p. 3522-6.
67. Xiao, H., et al., *The Toll-interleukin-1 receptor member SIGIRR regulates colonic epithelial homeostasis, inflammation, and tumorigenesis.* Immunity, 2007. **26**(4): p. 461-75.
68. Ben-Neriah, Y. and M. Karin, *Inflammation meets cancer, with NF-kappaB as the matchmaker.* Nat Immunol, 2011. **12**(8): p. 715-23.
69. Kain, V., S.D. Prabhu, and G.V. Halade, *Inflammation revisited: inflammation versus resolution of inflammation following myocardial infarction.* Basic Res Cardiol, 2014. **109**(6): p. 444.
70. Huang, J., et al., *Protective effect of the polarity of macrophages regulated by IL-37 on atherosclerosis.* Genet Mol Res, 2016. **15**(2).

71. Kumar, S., et al., *Interleukin-1F7B (IL-1H4/IL-1F7) is processed by caspase-1 and mature IL-1F7B binds to the IL-18 receptor but does not induce IFN-gamma production.* Cytokine, 2002. **18**(2): p. 61-71.
72. Ellisdon, A.M., et al., *Homodimerization attenuates the anti-inflammatory activity of interleukin-37.* Science Immunology, 2017. **2**(8).